Figure 3-27. Photograph of ash deposits on the CAH tubes following the January test firing Illinois No. 6 bituminous coal.

removed intact from the tube surfaces. The total weight of the deposits collected from the CAH tubes and duct was 14 lb (6.4 kg). The total weight of the deposits collected from the CAH tubes was 4 lb (1.8 kg). On a mass per unit time basis, the ash deposition rate for this Illinois No. 6 coal-fired test would be 0.07 lb/hr (30.3 g/hr) of coal firing. Incorporating the surface area of the tube bank (6.28 ft^2 or 0.58 m^2) results in a value of 0.01 lb/hr-ft^2 (52.2 g/hr-m^2). On a coal-firing-rate basis, the CAH ash deposition rate would be 0.03 lb/MMBtu (13.3 g/10^6 kJ). These calculated values are comparable to previous Illinois No. 6 tests.

Figures 3-28 through 3-30 summarize CAH tube bank surface and flue gas temperatures, process air temperatures, and process air flow rate data for the February test (SFS-RH7-0299). While natural gas was fired and the tubes were clean, heat recovery from the CAH tube bank was roughly 44,474 Btu/hr (46,921 kJ/hr). This result was observed for the following conditions:

- Process air flow rate of 127 scfm (3.6 m^3/min)
- Inlet process air temperature of 1010°F (544°C)
- Outlet process air temperature of 1195°F (646°C)
- Flue gas temperature of 1800°F (982°C) entering the CAH tube bank.

Figure 3-31 presents heat recovery in the CAH as a function of run time for the February test.

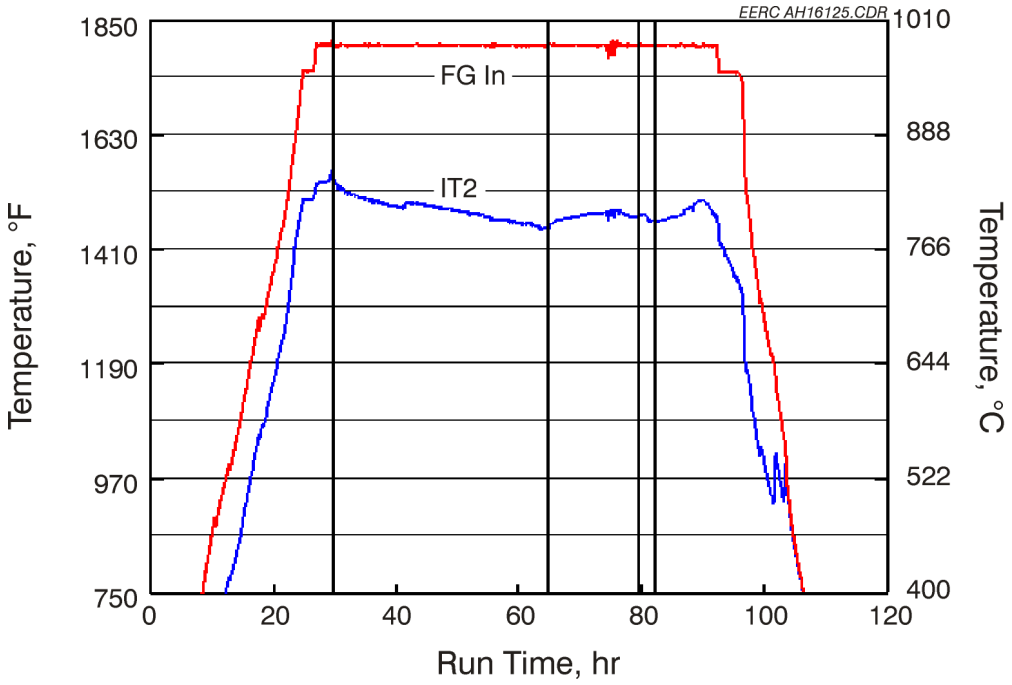

Figure 3-28. CAH tube surface and flue gas temperatures versus run time for the February test, SFS-RH7-0299.

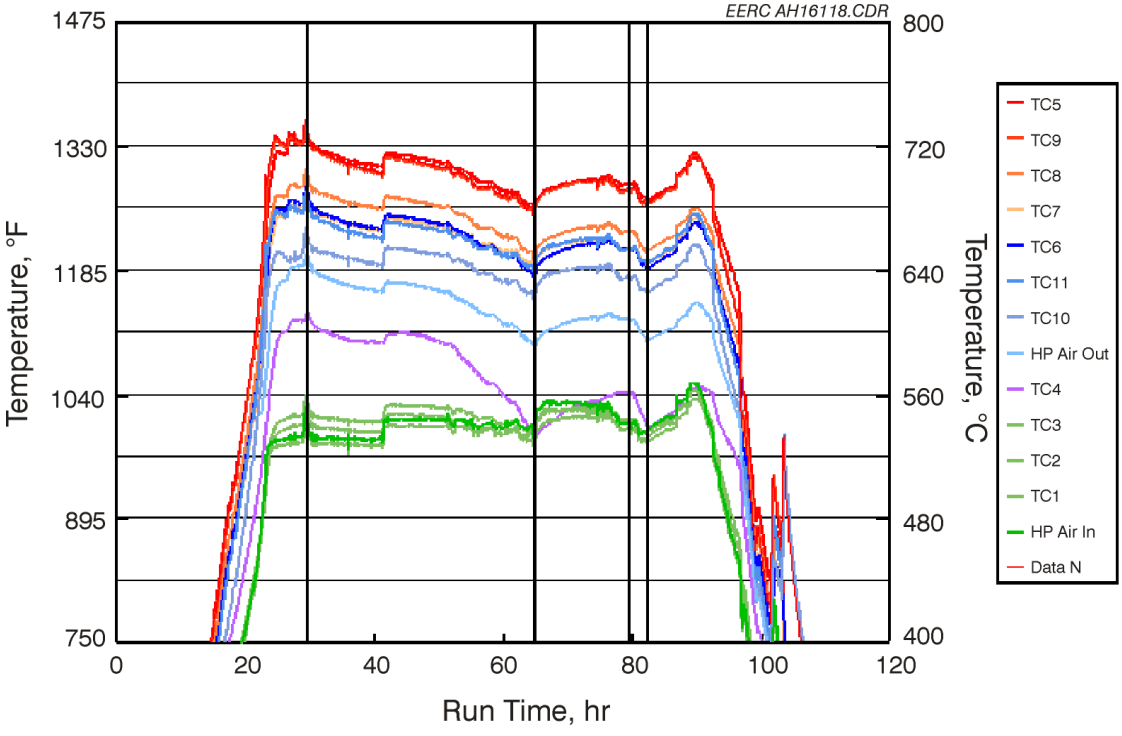

Figure 3-29. CAH process air temperatures versus run time for the February test, SFS-RH7-0299.

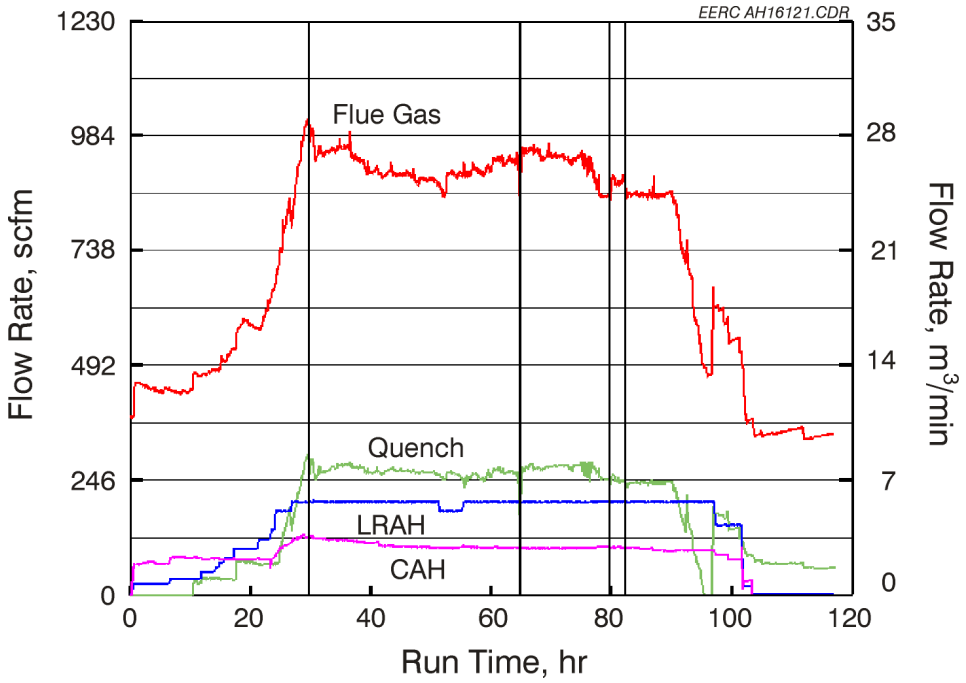

Figure 3-30. CAH process air, RAH process air, quench gas, and flue gas flow rates versus run time for the February test, SFS-RH7-0299.

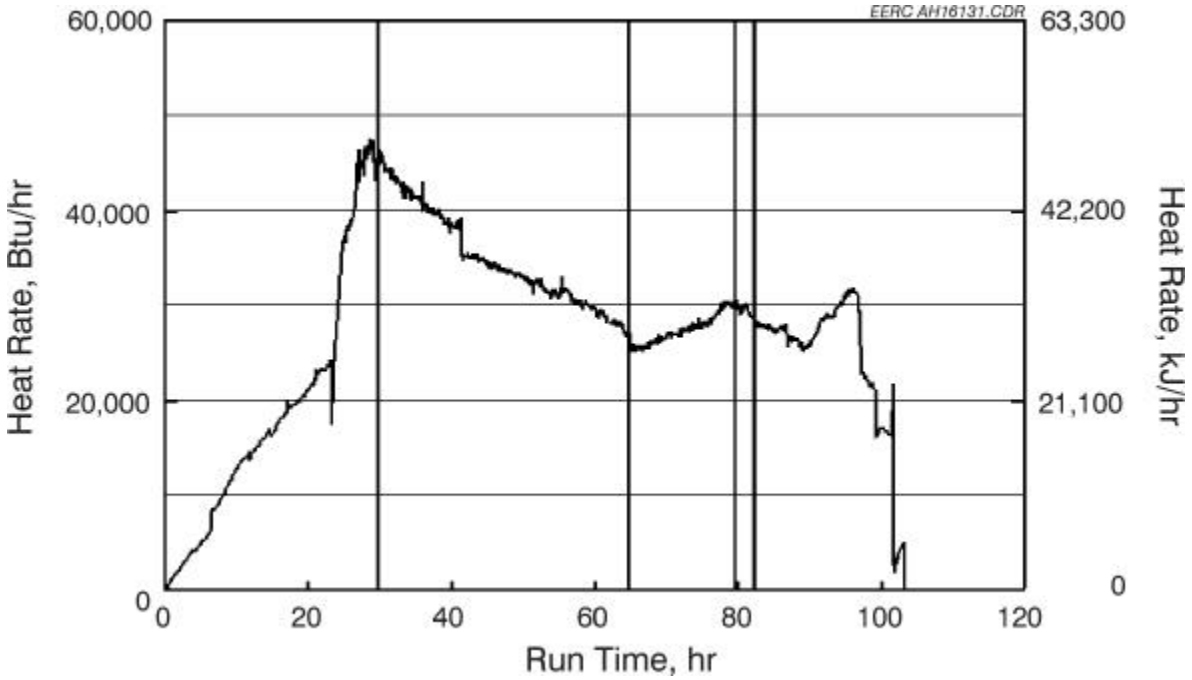

Figure 3-31. CAH heat recovery versus run time for the February test, SFS-RH7-0299.

When coal firing (Kentucky) began, surface temperatures initially decreased at a rate of nominally 5°F/hr (3°C/hr) over nearly 12 hours as ash deposits developed on the surface of the tubes. After nearly 40 hours of coal firing, there was no further decrease in tube surface temperature. It must be noted that process air flow rates were also decreasing (0.01 scfm/ 0.0003 m^3/min) over these time frames in an attempt to maintain a relatively constant process air exit temperature. The minimum process air flow rate through the CAH tube bank was 104 scfm (2.9 m^3/min). As ash deposits developed on the tube surfaces, heat recovery from the CAH tube bank decreased from roughly 46,500 Btu/hr (49,058 kJ/hr) to 27,000 Btu/hr (28,485 kJ/hr). The coal feed was terminated at this time because of the plugging problems in the slag screen. When coal feed resumed, heat recovery from the CAH tube bank was nominally 30,000 Btu/hr (31,650 kJ/hr). Heat recovery decreased to nominally 29,000 Btu/hr (30,595 kJ/hr) over the final 2.5 hours of coal firing prior to the termination of the coal feed. These data indicate that heat recovery from the CAH tube bank when the Kentucky bituminous coal was fired is significantly greater as compared to the Illinois No. 6 coal data. This result is most likely due to the smaller quantity of ash in the Kentucky fuel and the differences in ash properties.

EERC personnel did not clean the CAH tube bank during the February test in order to facilitate the development of ash deposits for characterization. CAH tube bank plugging was not a problem. No deposits were observed bridging the flue gas paths between the tubes. The deposits that formed were limited to the leading and trailing edges of the tubes. In addition, these deposits did not bridge the area between the tubes in the direction of the flue gas flow as was observed when the Illinois No. 6 coal was fired.

Figure 3-32 presents a photograph of ash deposits on the surface of the tubes following the February test. The photograph shows three of the five uncooled tubes as well as two of the seven air-cooled finned tubes. The leading- and trailing-edge deposits are readily visible, with very little ash present on the side walls of either the uncooled or cooled metal surfaces. There do not appear to be any pieces of tube deposit missing in the photograph.

Deposit strength is a function of ash chemistry, particle size, and temperature history. The deposits remained intact when the CAH tube bank was removed from the duct. However, the small quantity of deposit and, therefore, minimal weight may have been the primary reason the deposit remained intact when the tube bank was removed from the duct. Also, the deposits from the cooled tubes were not generally removed intact from the tube surfaces. The total weight of the deposits collected from the CAH tubes and duct was 2.2 lb (1.0 kg). The total weight of the deposits collected from the CAH tubes was 1 lb (0.5 kg). On a mass per unit time basis, the ash deposition rate for this Kentucky coal-fired test would be 0.03 lb/hr (13.6 g/hr) of coal firing. Incorporating the surface area of the tube bank (6.28 ft^2 or 0.58 m^2) results in a value of 0.005 lb/hr-ft^2 (23.4 g/hr-m^2). On a coal-firing-rate basis, the CAH ash deposition rate would be 0.01 lb/MMBtu (5.9 g/10^6 kJ). These calculated values are nominally a factor of 3 smaller than those observed for the Illinois No. 6 coal, consistent with the Kentucky coal's lower ash content and higher heating value.

Table 3-8 shows the compositions of the deposits that formed on both the uncooled dummy tubes and the cooled tubes during the February test. The compositions show that, like the slag

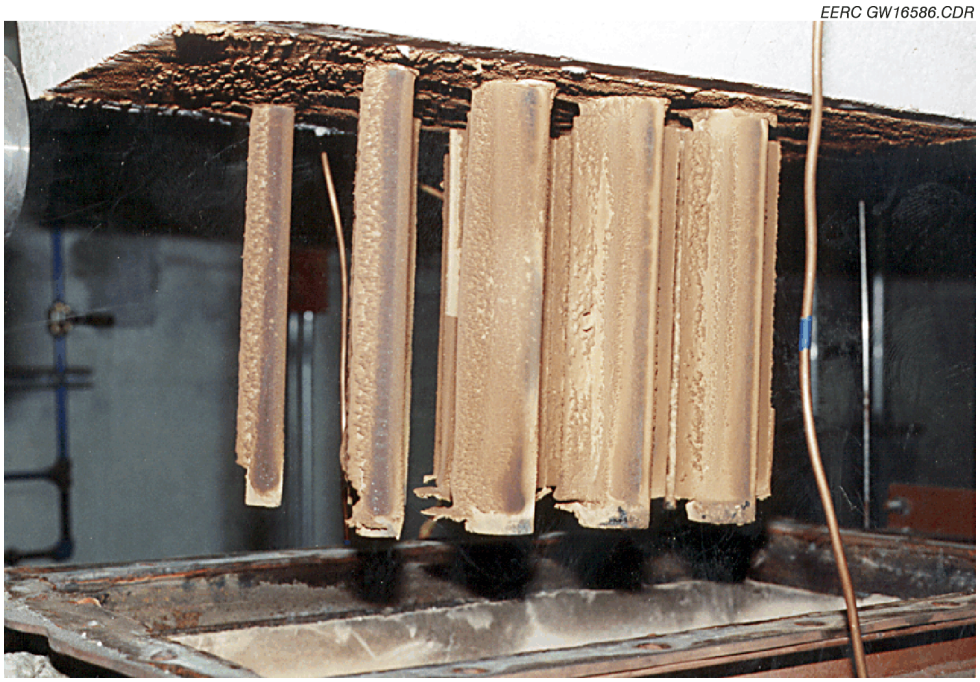

Figure 3-32. Photograph of ash deposits on the CAH tubes following the February test firing eastern Kentucky bituminous coal.

TABLE 3-8

CAH Deposit Samples from the February Test

Oxides,[1] wt%	Kentucky Coal	Uncooled Front	Uncooled Back	Cooled Front	Cooled Back
SiO_2	40.4	53.5	52.1	53.2	53.2
Al_2O_3	30.8	20.1	20.7	20.7	20.6
Fe_2O_3	10.6	14.1	14.2	14.5	14.1
TiO_2	1.1	1.2	1.3	1.3	1.3
P_2O_5	0.1	0.2	0.4	0.3	0.3
CaO	10.9	4.4	2.4	3.3	2.4
MgO	2.3	1.8	1.8	1.8	1.9
Na_2O	1.5	1.8	3.0	1.8	2.5
K_2O	2.3	2.8	4.2	3.1	3.8
SO_3[2]	6.7	0.3	0.2	1.0	0.4

[1] Oxide concentrations normalized to an SO_3-free basis.
[2] SO_3 concentrations normalized with other oxides.

collected in the slag screen, the deposits are dominated by larger particles enriched in silica and iron and depleted in alumina and calcia. It is unusual that the compositions of the upstream and downstream deposits are so similar, since the upstream deposits are usually more enriched with

larger particles and the downstream deposits usually more enriched with smaller particles. SEM analyses showed that essentially all of the different deposits were composed of complex silicates, except for a thin powder layer adjacent to the tube, which contained approximately 15% sulfate material.

Figures 3-33 through 3-35 summarize CAH tube bank surface and flue gas temperatures, process air temperatures, and process air flow rate data for the April test (SFS-RH8-0399). While natural gas was fired and the tubes were clean, heat recovery from the CAH tube bank was roughly 40,000 Btu/hr (42,200 kJ/hr). This result was observed for the following conditions:

- Process air flow rate of 111 scfm (3.1 m^3/min)
- Inlet process air temperature of 1080°F (582°C)
- Outlet process air temperature of 1270°F (688°C)
- Flue gas temperature of 1790°F (977°C) entering the CAH tube bank.

Figure 3-36 presents heat recovery in the CAH as a function of run time for the April test.

When coal firing (eastern Kentucky) began, surface temperatures initially decreased at a rate of nominally 5°F/hr (3°C/hr) over nearly 10 hours as ash deposits developed on the surface of the tubes. After 40 hours of coal firing, the rate of decrease was 0.7°F/hr (0.4°C/hr). No

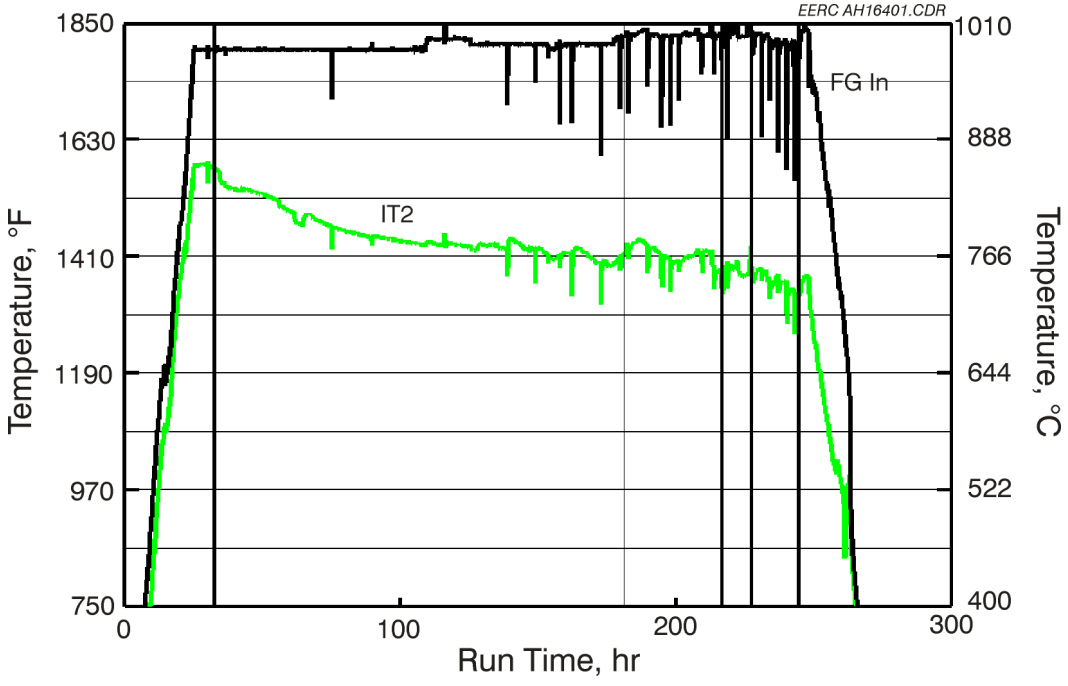

Figure 3-33. CAH tube surface and flue gas temperatures versus run time for the April test, SFS-RH8-0399.

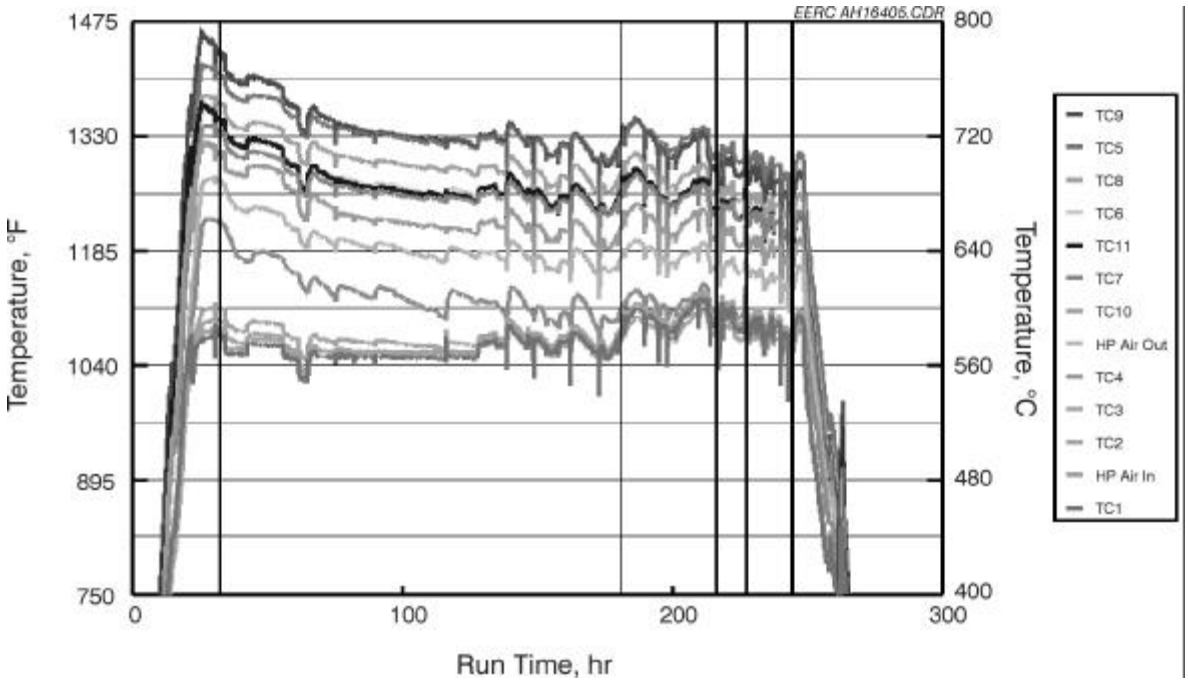

Figure 3-34. CAH process air temperatures versus run time for the April test, SFS-RH8-0399.

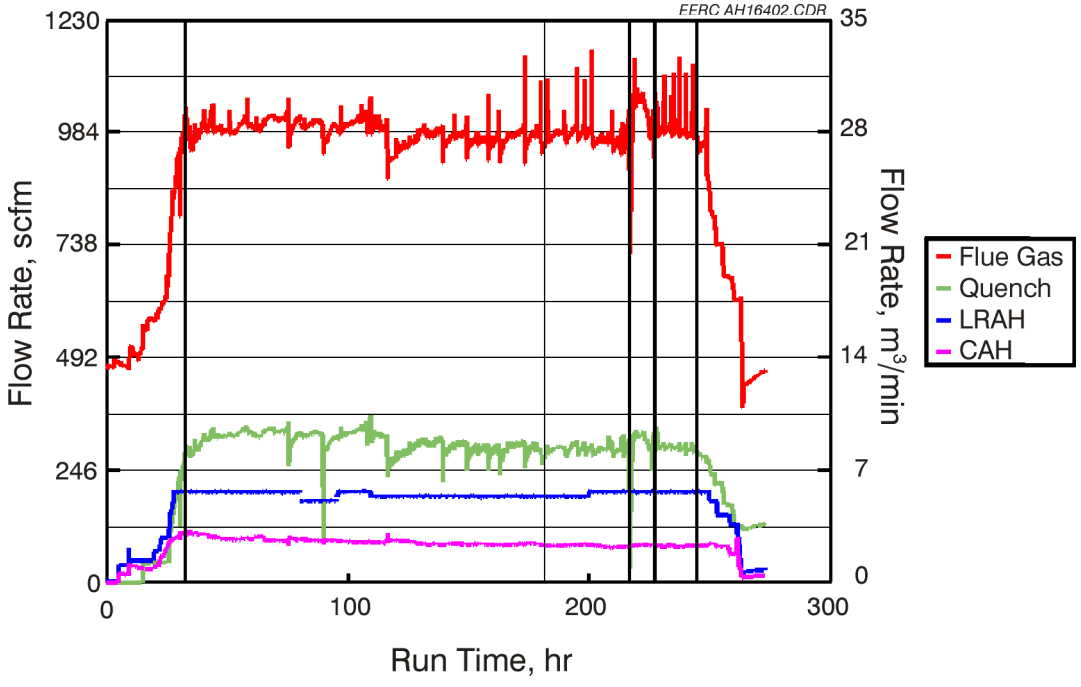

Figure 3-35. CAH process air, RAH process air, quench gas, and flue gas flow rates versus run time for the April test, SFS-RH8-0399.

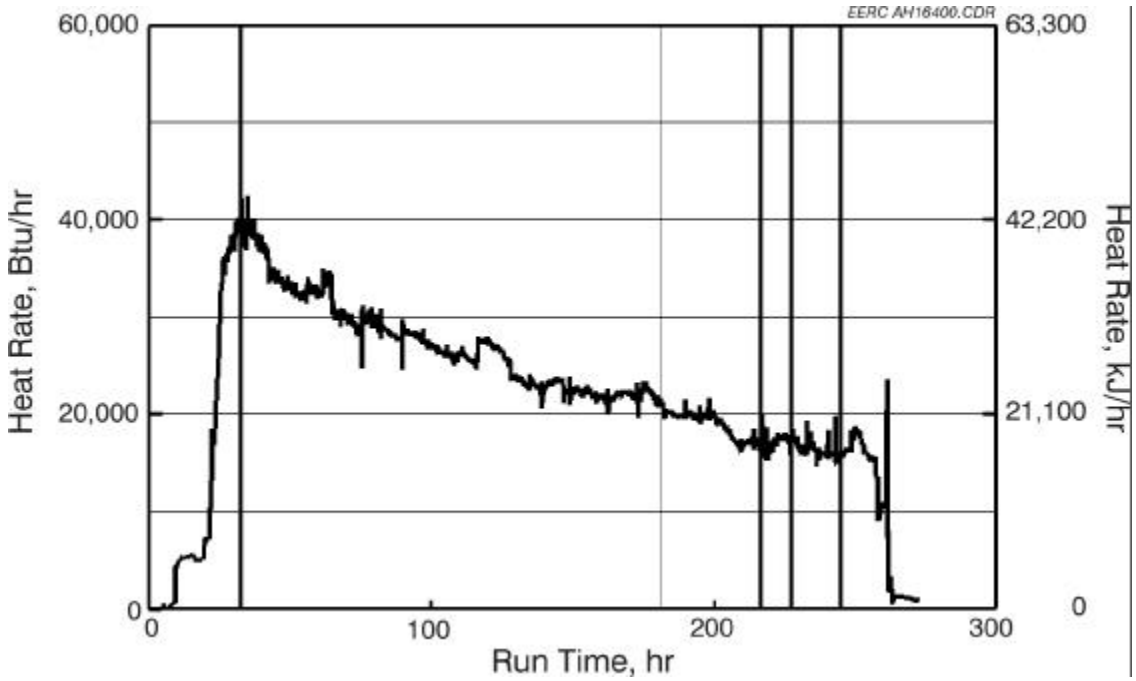

Figure 3-36. CAH heat recovery versus run time for the April test, SFS-RH8-0399.

further decrease in tube surface temperature was noted, other than changes related to flue gas flow rates, flue gas temperatures, process air flow rates, and process air temperatures, until the eastern Kentucky coal was replaced by the Illinois No. 6 coal. It must be noted that process air flow rates were also decreasing (0.1 scfm/0.003 m^3/hr) over these time frames in an attempt to maintain a relatively constant process air exit temperature. The minimum process air flow rate through the CAH tube bank was 77 scfm (2.2 m^3/min). As ash deposits developed on the tube surfaces, heat recovery from the CAH tube bank decreased from roughly 40,000 Btu/hr (42,200 kJ/hr) to 21,200 Btu/hr (22,366 kJ/hr) when the eastern Kentucky coal was fired. Heat recovery from the CAH tube bank remained at this level for nearly 42 hours prior to the switch to the Illinois No. 6 coal. One reason for the steady heat recovery rate may have been spontaneous shedding of the ash-fouling deposits from the CAH tubes, as indicated by piles of ash at the bottom of the tubes. As shown in Table 3-8, the CAH deposits formed when the eastern Kentucky coal was fired contained around 50% silica, and all alkali and alkaline-earth species were present in very low concentrations, so limited sintering at the temperatures of the CAH would be expected.

Over the final 51 hours of coal firing (Illinois No. 6), the heat recovery from the CAH tube bank decreased and eventually stabilized at 16,000 Btu/hr (16,880 kJ/hr) prior to termination of the coal feed. These data are generally consistent with the February test firing eastern Kentucky coal as well as previous tests firing Illinois No. 6 coal. A comparison of the results shows a nominal 30% higher heat recovery rate in the CAH tube bank when the eastern Kentucky coal is fired, probably because of spontaneous ash deposit shedding. However, these data do not address

the potential for improved heat recovery for either fuel type as a function of an effective sootblowing system.

These data continue to support the conclusion that the addition of the fins to the air-cooled tubes improves heat recovery during the coal-fired test periods. The fins appear to reduce the rate of heat-transfer degradation as ash deposits developed and help to maintain a higher heat-transfer rate once the deposits have formed. However, no improvement in heat recovery is observed during the initial natural gas-fired periods with clean tube surfaces.

EERC personnel did not clean the CAH tube bank during the April test, and ash deposits were not characterized as a result of the need to switch fuels during the 200-hour test. CAH tube bank plugging was not a problem. No deposits were observed bridging the flue gas paths between the tubes. The deposits that formed were limited to the leading and trailing edges of the tubes. However, these deposits did bridge the area between the tubes in the direction of the flue gas flow. Deposit bridging between tubes in the direction of the flue gas flow may have been the result of a longer eastern Kentucky coal-fired period or occurred as a result of firing the Illinois No. 6 coal during the last 51 hours. EERC personnel believe the latter scenario more likely. Future SFS tests should answer this question.

Figure 3-37 presents a photograph of ash deposits on the surface of the tubes following the April test. The photograph shows three of the five uncooled tubes as well as two of the seven air-cooled finned tubes. The leading- and trailing-edge deposits are readily visible, with bare metal surfaces visible on the back half of the uncooled tubes. The pieces of tube deposit missing from

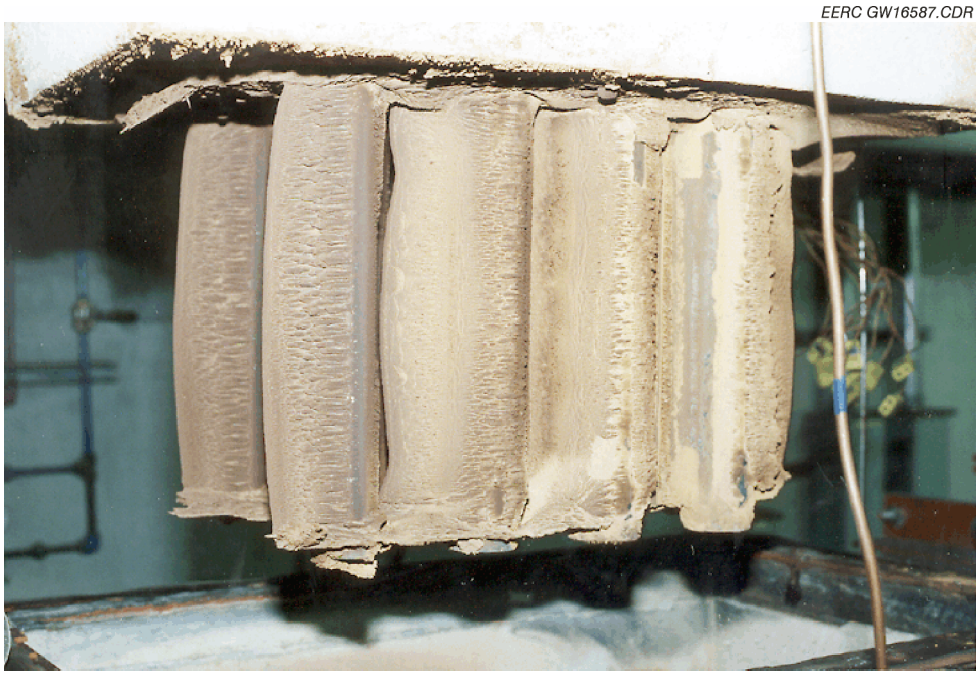

Figure 3-37. Photograph of ash deposits on the CAH tubes following the April test firing eastern Kentucky and Illinois No. 6 bituminous coal.

the photograph of the air-cooled tubes fell off as the tube bank was removed from the duct. Because two different fuels were fired during this test, a discussion of deposit strength, weight, and deposition rate is not warranted.

3.1.3 RAH Panel Performance

RAH panel performance was excellent during the test periods completed in support of this project. Heat transfer was better than previously observed. No ceramic tile failures occurred, although tile cracking occurred as a result of thermal cycles. Process air temperatures of 1625° to 1800°F were achieved and controlled at the RAH exit based on process air flow rate.

Initial shakedown and testing of the RAH panel took place in December 1997. Testing of the RAH panel continued in January, February, and April 1999 following its reassembly in early January. Reassembly of the RAH panel was necessary because of ceramic tile failures in August 1998. The primary purpose of the January, February, and April tests was to further evaluate the RAH panel performance relative to heat transfer, tile and tube temperatures, and process air temperatures and flow rates. In addition, a critical aspect of RAH panel performance is the ability of the ceramic tiles to withstand the slag attack and thermal cycling conditions in the slagging furnace. Generally, the performance of the RAH panel during the three test periods discussed in this report was as anticipated, with no significant process or material problems observed.

The RAH panel ceramic tiles were thoroughly inspected upon initial installation and following each week of operation. The initial inspection revealed the presence of minor cracks in two of the five ceramic tiles. Cracks were not visible in either of the top or bottom support blocks. Figure 3-38 is a photograph of the new ceramic tiles installed on the RAH panel inside of the slagging furnace prior to the January 1999 test. The cracks visible at the time were hairline cracks in the large upper and lower tiles. The large upper tile had five visible cracks originating from the left edge and one crack originating from the top edge. Cracks originating from the left edge were about 0.75 in. (1.9 cm) in length and are not visible in the photograph. The vertical crack is visible in the photograph as a result of the application of a blue die. In addition, rough surface pitting of the tile is evident at the end of the vertical crack in the upper center of the tile. The large lower tile had one crack originating on the left edge and a few rough surface pits along the right edge near the middle of the tile. Neither the crack nor the surface pits in the large lower tile are visible in the photograph.

The cracks found in new tiles are believed to result from stresses encountered during tile fabrication, the actual casting/cooling process, and the machining of the tiles. These stresses and the resulting cracks could be reduced if the tiles could be formed in near net shapes, eliminating the need for machining. Work in this area is progressing within the Combustion 2000 HiPPS program.

Figure 3-39 presents photographs of the furnace interior after the January (top) and February (bottom) tests. Both photographs illustrate the excellent condition of the high-density furnace refractory as well as the darkening of the refractory with exposure to slag as a result of coal firing. Exposure of the RAH ceramic tiles to slag during coal firing in January darkened the

Figure 3-38. Photograph of new ceramic tiles installed on the RAH panel inside of the slagging furnace in January 1999.

tiles as a result of the residual slag layer on the surface. No additional tile color change is evident following the February test. Although not obvious in the photos, the slag layer on the tiles is thin and appears to be uniform with no evidence of any extensive slag buildup. While there was some slag present in the seams between the tiles, there was no evidence of any fusion between adjacent tiles. Therefore, the 4-hour period of natural gas firing prior to SFS cooldown appears to be adequate to prevent buildup of excess slag on the surface of the tiles or in the seams between tiles for the Illinois No. 6 and Kentucky bituminous coals. Also, any quantity of slag present in the seams between tiles appears to crack as a result of cooldown and tile movement.

Figure 3-40 presents a photograph of the furnace interior after the April test and illustrates the good condition of the high-density furnace refractory as well as the darkening of the refractory with exposure to slag. With each week of coal firing, the high-density furnace refractory gets darker. The high-density refractory immediately below the RAH panel is showing signs of deterioration as a result of slag dripping off the bottom RAH support brick onto the refractory.

Figure 3-41 illustrates the visible cracks found in the RAH tiles following the January (left) and February (right) tests. Overall, the tiles appear to be in good condition. Following the January test, visible cracks were only evident in two tiles, the small and large upper tiles. The small crack evident in the large lower tile prior to coal firing was covered with slag and was not evident following the January test. One crack was evident in the small upper tile following the January test. The crack originated on the left edge and was <3 in. (<7.6 cm) in length. Six cracks

Figure 3-39. Photographs of the RAH panel inside of the slagging furnace following the January (top) and February (bottom) tests.

Figure 3-40. Photograph of the RAH panel inside of the slagging furnace following the April test.

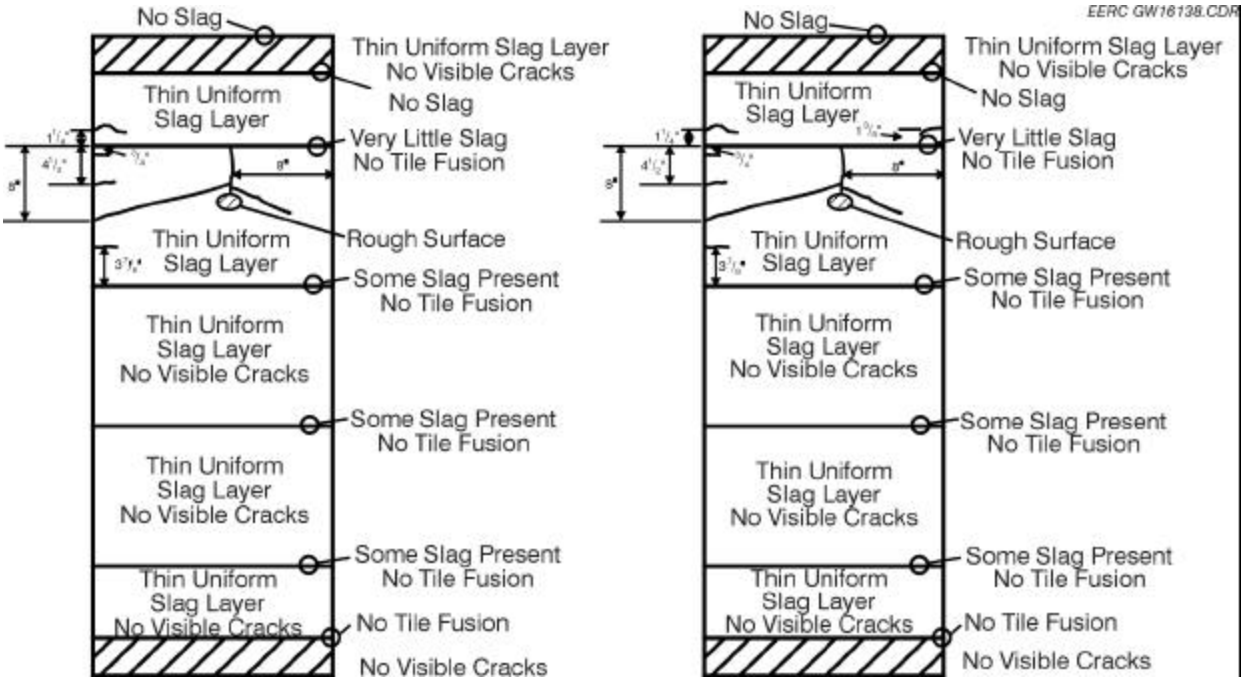

Figure 3-41. Illustrations of cracks found in the ceramic tiles/bricks of the RAH panel after testing in January (left) and February (right) 1999.

were visible in the large upper tile following the January test, four originating from the left edge, one from the top edge, and one originating from the area of the rough surface pits and extending down toward the right edge. The four cracks originating from the left edge were visible prior to exposure of the tile to furnace conditions. However, one of the cracks had grown in length and intersected the vertical crack originating from the top edge. A fifth crack that had been observed originating from the left edge prior to tile exposure to furnace conditions was not evident after the January and February tests as a result of slag covering the tile. The vertical crack in the large upper tile does not appear to have changed as a result of the January and February tests. However, the combination of the vertical crack, the crack extending from the left edge, and the new crack extending toward the right edge could be problematic with further heating and cooling cycles. The only other change in tile cracking that was observed following the February test was the appearance of a new crack originating on the lower right edge of the small upper tile.

Figure 3-42 illustrates the visible cracks found in the RAH tiles following the April test. Overall, the condition of the tiles deteriorated somewhat with each test, with the small lower tile showing the greatest degree of erosion/corrosion. This is believed to result from the combination of its higher surface temperature and the greater quantity of slag flowing over its surface relative to the other tiles. The surface temperature of the small lower tile, although not measured, is believed to be higher than the three larger tiles because the backside of this tile is insulated within the radiation cavity and is not directly cooled by the heat-transfer surfaces. The greatest quantity of slag also flows over this tile because of its location below the other tiles.

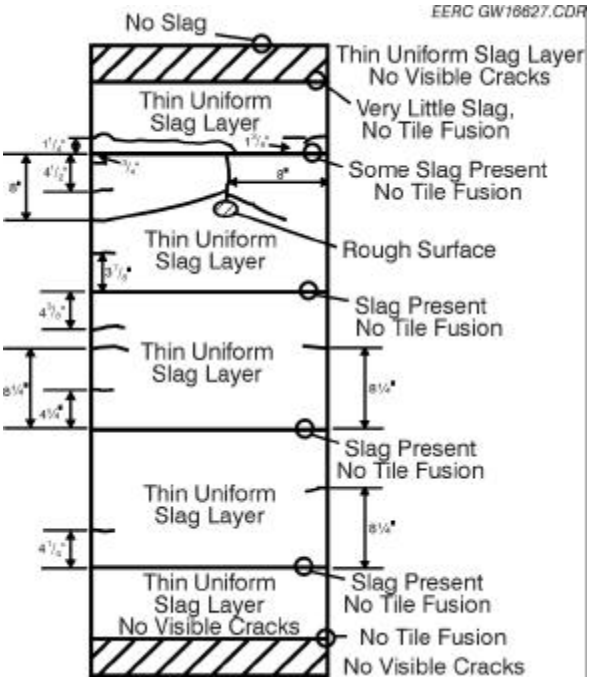

Figure 3-42. Illustration of cracks found in the ceramic tiles/bricks of the RAH panel after testing in April 1999.

The cracks in the large lower and middle tiles were hairline cracks posing no concern following the April test. The large upper tile had the most extensive cracking and, therefore, poses a concern with respect to potential failure. The five cracks originating from the left edge were visible prior to exposure of the tile to furnace conditions, although one of the cracks has grown in length and intersects the vertical crack originating from the top edge. The vertical crack in the large upper tile does not appear to have changed as a result of the April test. However, the combination of cracks in the large upper tile could be problematic with further heating and cooling cycles.

Heatup/cooldown cycles are believed to be the primary cause of RAH panel ceramic tile/brick cracking and the propagation of cracks formed during tile fabrication, with slag contributing to erosion/corrosion of surfaces and imparting stresses on the ceramic tile as it finds its way into seams between tiles. Figure 3-43 is a photograph of the lower support brick, small lower tile, and the lower edge of the large lower tile following the February test. Figure 3-44 presents a photograph of the RAH panel from inside of the furnace following the April test. Both photographs show where the flow of slag has caused erosion/corrosion of the tile surfaces. This observation is consistent with those made concerning the original RAH tiles installed in December 1997 and removed subsequent to failure in August 1998. In addition, the photographs illustrate the small quantity of slag found in the seams between the tiles.

Figures 3-45 through 3-47 summarize the RAH ceramic tile temperatures, tube surface temperatures, and process air temperatures for the January test (SFS-RH6-0199). The process air flow rate data for the RAH panel were summarized in Figure 3-24. Figure 3-48 illustrates the

Figure 3-43. Photograph of the RAH lower support brick, small lower tile, and the lower edge of the large lower tile following the February test.

Figure 3-44. Photograph of the RAH panel from inside of the furnace following the April test.

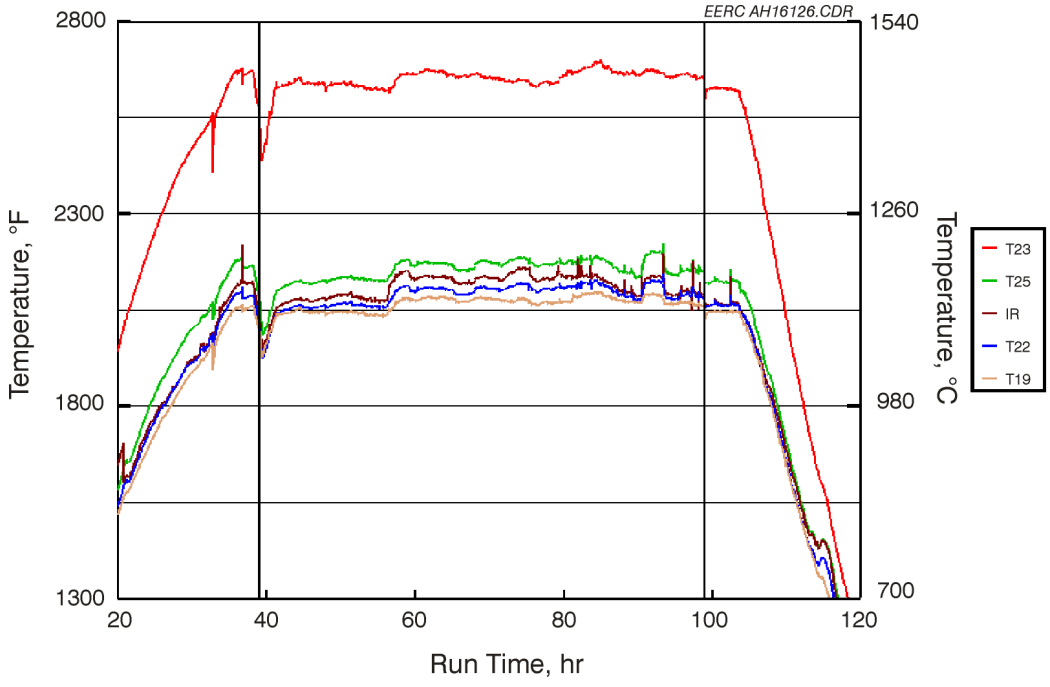

Figure 3-45. RAH ceramic tile temperatures versus run time for the January test, SFS-RH6-0199.

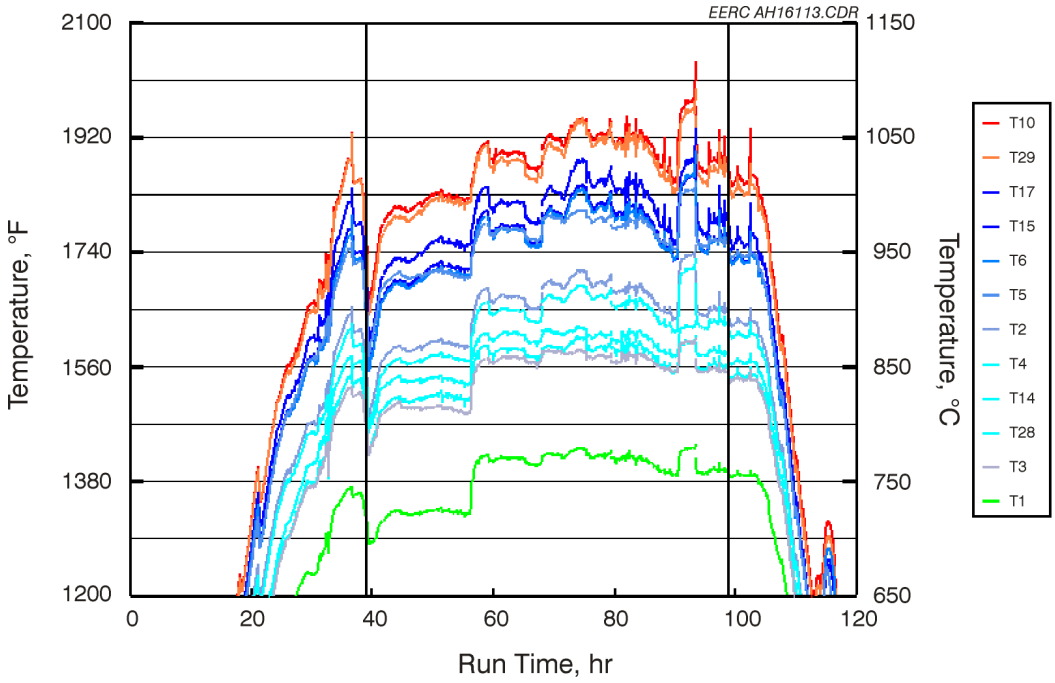

Figure 3-46. RAH tube surface temperatures versus run time for the January test, SFS-RH6-0199.

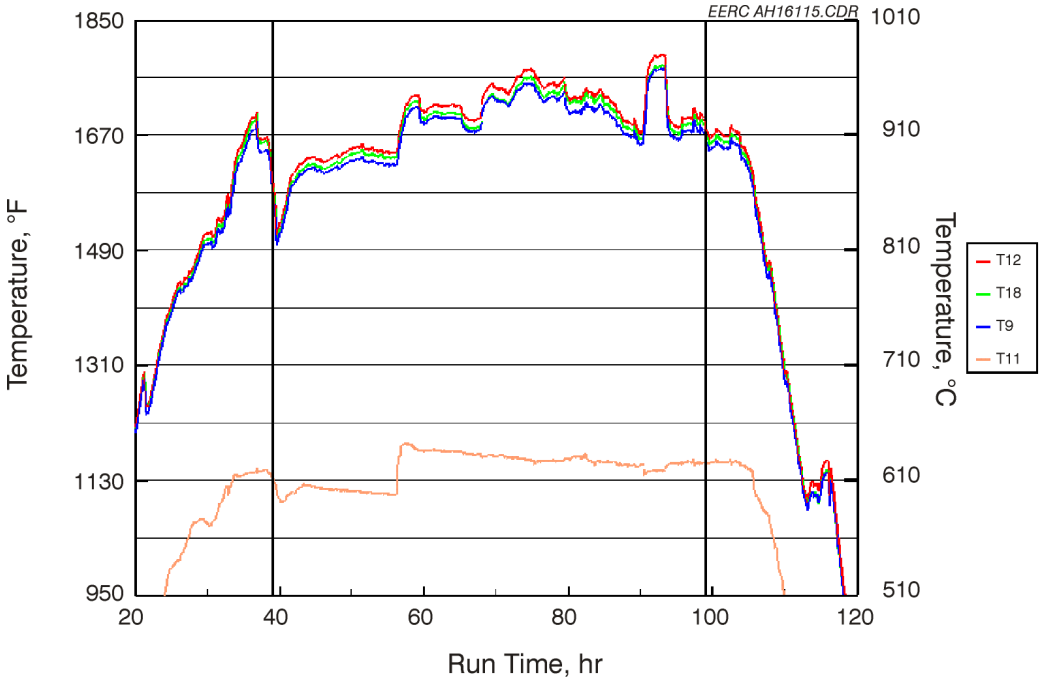

Figure 3-47. RAH process air temperatures versus run time for the January test, SFS-RH6-0199.

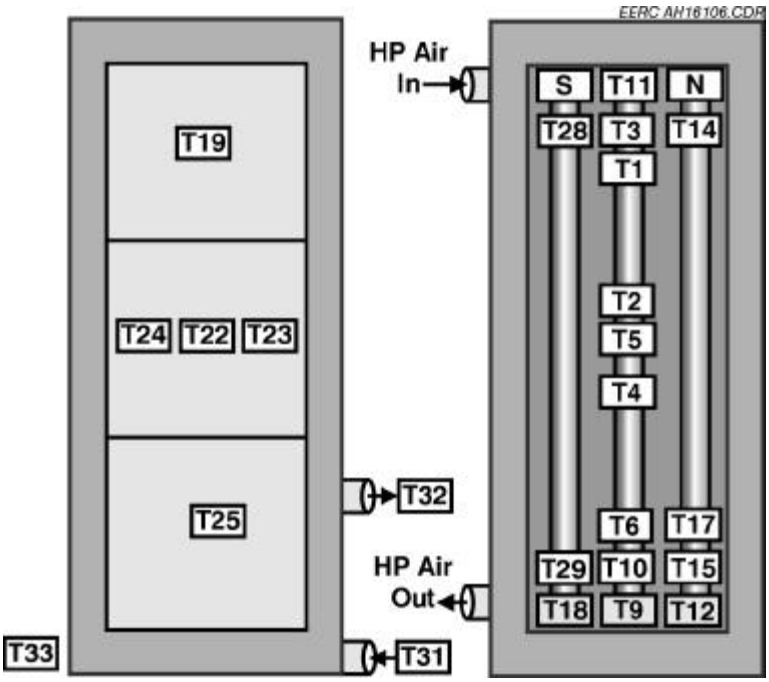

Figure 3-48. Thermocouple locations in the RAH Panel.

location of thermocouples in the RAH panel, and Table 3-9 describes the RAH thermocouples. The indicated ceramic tile surface temperatures (cavity-side) ranged from nominally 2040° to 2205°F (1116° to 1208°C), based on measurements made at the center of each of the three large tiles once the SFS had stabilized thermally (Run Hours 45 through 99). Higher tile surface temperatures (furnace-side), 2620° to 2693°F (1438° to 1479°C), were measured near the center of the large middle tile. Tile surface temperatures during the January test were somewhat higher yet comparable to the temperatures observed during the first RAH coal-fired test completed in December 1997. However, the furnace-side tile temperature is a new thermocouple location. Therefore, a direct comparison with previous data is not appropriate.

RAH process air flow rates during the January test were controlled at 150, 180, 200, 205, and 220 scfm (4.2, 5.1, 5.7, 5.8, and 6.2 m^3/min), with 200 scfm (5.7 m^3/min) used primarily. Changes in process air flow rates had a definite effect on indicated tile surface temperatures. As process air flow rates were reduced, tile surface temperature increased. Subsequently, when process air flow rates were increased, tile surface temperatures decreased. This effect is most evident for process air flow rate changes at Run Hours 68, 79, 90, and 93.

RAH tube surface temperatures ranged from nominally 1330° to 1970°F (721° to 1077°C). The low end of the temperature range represents the back side of the tube surfaces near the process air inlet, with the high end of the temperature range representing the front side of the tube surfaces near the process air outlet. Changes in process air flow rates had noticeable effects on all tube surface temperatures. Tube surface temperature step changes were most noticeable for surface temperature measurements near the process air exit and on the front side of the tubes.

TABLE 3-9

Description of RAH Panel Thermocouple Locations[1]

Category	No.	Label	Description
Air Inlet	1	HP Air In	Provided by the EERC, in pipe before inlet header
	2	RAHT11	Air entering RAH through center tube
Air Outlet	3	RAHT18	Air leaving left (south) tube
	4	RAHT9	Air leaving middle tube
	5	RAHT12	Air leaving right (north) tube
MA Tube Surface	6	RAHT1	Top of middle tube facing cold side
	7	RAHT2	Middle of middle tube facing other tube
	8	RAHT3	Top of middle tube facing toward furnace
	9	RAHT4	Middle of middle tube facing cold side
	10	RAHT5	Middle of middle tube facing toward furnace
	11	RAHT6	Bottom of middle tube facing cold side
	12	RAHT7	Removed
	13	RAHT8	Removed
	14	RAHT10	Bottom of the middle tube facing toward furnace
	15	RAHT13	Removed
	16	RAHT14	Top of north tube facing toward furnace
	17	RAHT15	Bottom of north tube facing toward furnace
	18	RAHT16	Removed
	19	RAHT17	Bottom of north tube facing toward side wall
	20	RAHT28	Top of south tube facing toward furnace
	21	RAHT29	Bottom of south tube facing toward furnace
Inner Surface of Monofrax bricks	22	RAHT19	Top tile, center
	23	RAHT20	Removed
	24	RAHT21	Removed
	25	RAHT22	Middle tile, center
	26	RAHT23	Middle tile, right center hot-side surface
	27	RAHT24	Middle tile, left side rail
	28	RAHT27	Removed
	29	RAHT25	Lower tile, center
	30	RAHT26	Removed

[1] Thermocouple locations are illustrated in Figure 3-48.

Tube surface temperatures in January were comparable to all previous bituminous coal-fired tests.

Heat recovery data from the RAH panel are presented in Figure 3-49 for the January test. At process air flow rates of 150, 180, and 200 scfm (4.2, 5.1, and 5.7 m^3/min), the heat recovered from the RAH panel during coal firing was 120,000 Btu/hr (126,600 kJ/hr), 125,960 to 136,540 Btu/hr (132,888 to 144,050 kJ/hr), and 128,850 to 144,230 Btu/hr (135,937 to 152,163 kJ/hr), respectively. For process air flow rates of 180 and 200 scfm (5.1 and 5.7 m^3/min),

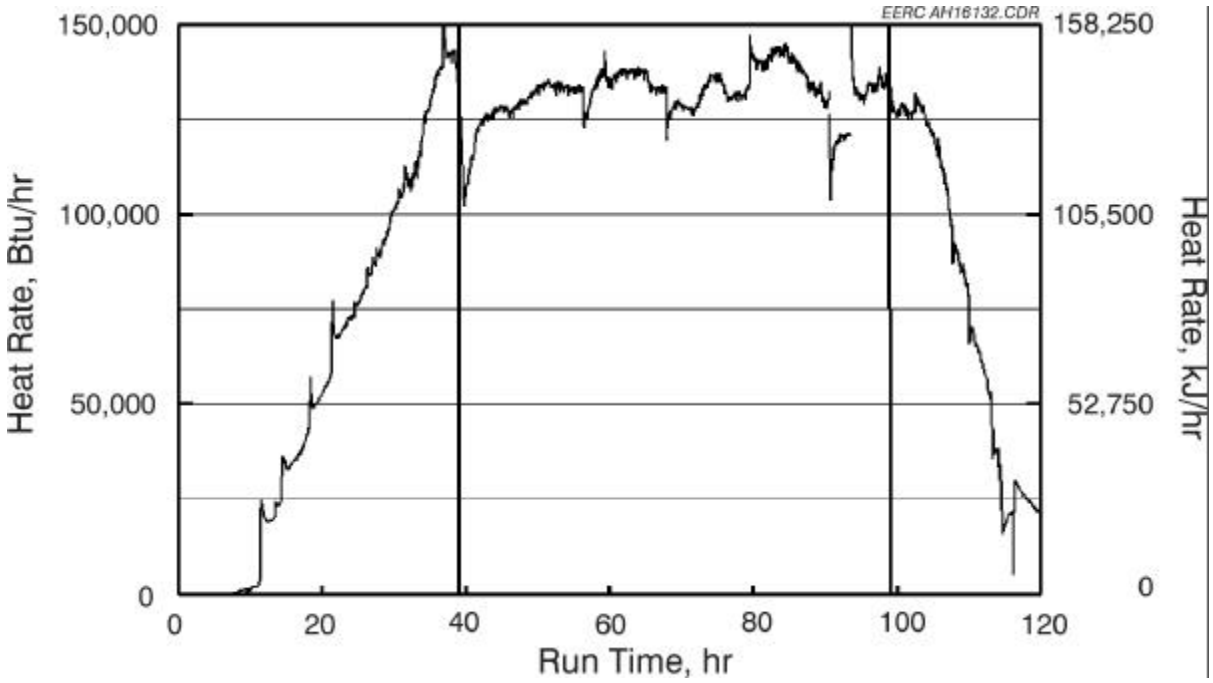

Figure 3-49. RAH heat recovery versus run time for the January test, SFS-RH6-0199.

the heat recovery ranges are a function of minor adjustments to the coal feed rate, combustion air flow rates, and main burner swirl setting. The main burner firing rate was nominally 2.1 to 2.25 MMBtu/hr (2.2 to 2.3 × 10^6 kJ/hr).

A comparison of the RAH panel data for the January Illinois No. 6 bituminous coal-fired test and the previous tests firing the same fuel indicates that there has been a significant improvement in the heat recovery rate. During previous test periods, the heat recovery rate in the RAH panel was <120,000 Btu/hr (<126,600 kJ/hr). However, in January, the heat recovery rate was generally >120,000 Btu/hr (>126,600 kJ/hr). The higher heat recovery rate observed in January was potentially a function of many factors: 1) the SRAH panel was no longer in place, 2) a minimal main burner swirl setting resulted in a more uniform temperature over the length of the furnace, 3) the total furnace firing rate was somewhat higher in January than tests completed in late 1997 and early 1998, and 4) the new condition of the high-density refractory may have resulted in a slight reduction in furnace heat loss. Another possible contributing factor may have been the position of the inlet and outlet process air thermocouples. These thermocouples were reinstalled in January when the RAH panel was reassembled. Although every effort was made to place the thermocouples in exactly the same position they had previously occupied, it is possible that the measurement location was altered slightly. Further testing and data review would be necessary to develop an explanation for the higher RAH heat recovery observed in January.

Figures 3-50 through 3-52 summarize the RAH ceramic tile temperatures, tube surface temperatures, and process air temperatures for the February test (SFS-RH7-0299). The process air flow rate data for the RAH panel were summarized in Figure 3-30. Once the SFS had

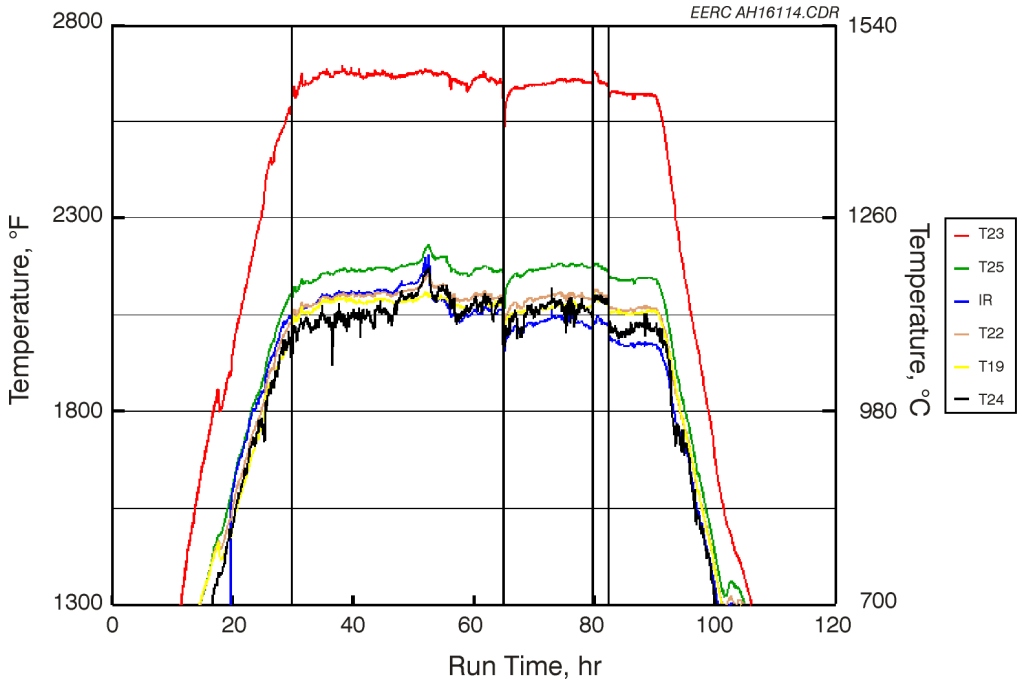

Figure 3-50. RAH ceramic tile temperatures versus run time for the February test, SFS-RH7-0299.

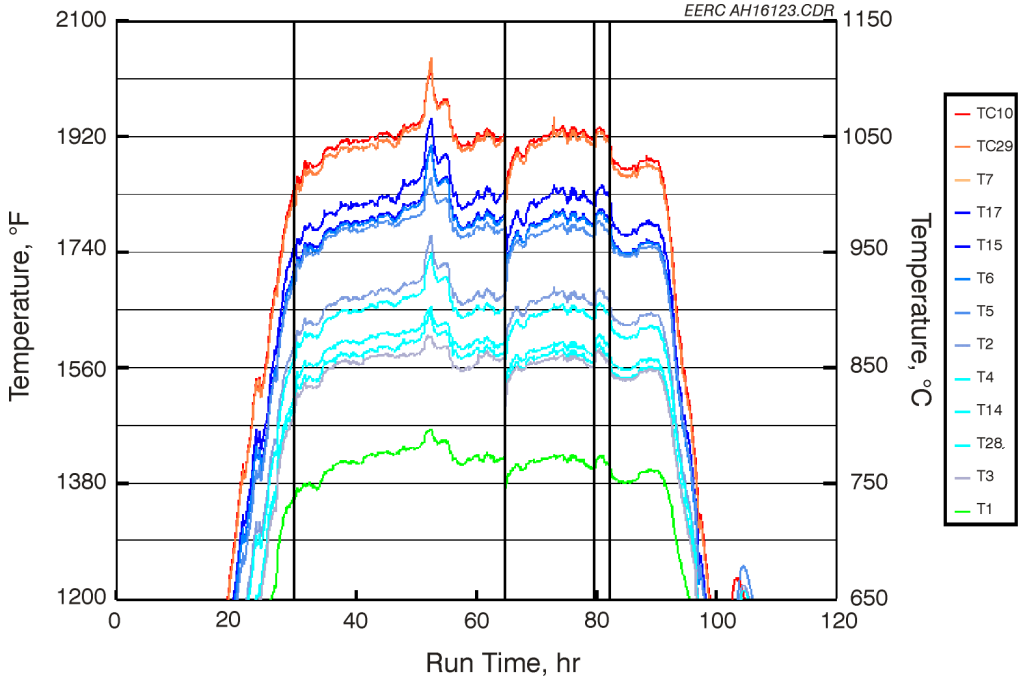

Figure 3-51. RAH tube surface temperatures versus run time for the February test, SFS-RH7-0299.

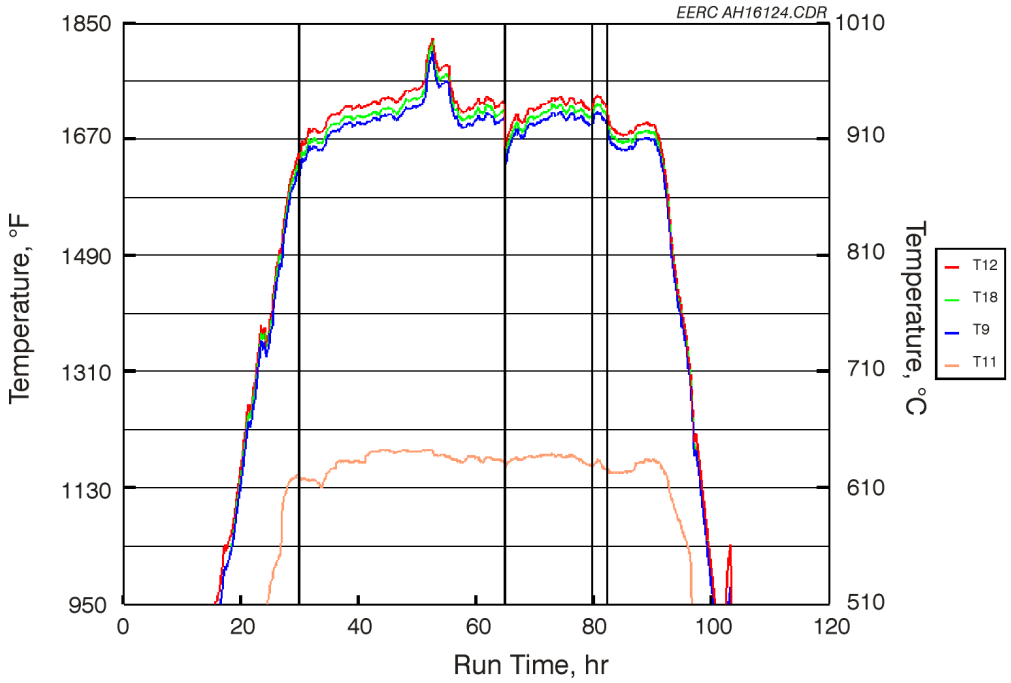

Figure 3-52. RAH process air temperatures versus run time for the February test, SFS-RH7-0299.

stabilized thermally (Run Hours 35 through 65 and 80 through 82), the indicated ceramic tile surface temperatures (cavity side) ranged from nominally 2070° to 2170°F (1133° to 1188°C), on the basis of measurements made at the center of each of the three large tiles. Higher tile surface temperatures (furnace-side), 2640° to 2690°F (1449° to 1477°C), were measured near the center of the large middle tile. Tile surface temperatures during the February test were comparable to those observed in January.

RAH process air flow rates during the February test were controlled at 180 and 200 scfm (5.1 and 5.7 m^3/min), with 200 scfm (5.7 m^3/min) used primarily. Changes in process air flow rates had a definite effect on indicated tile surface temperatures as observed for the January test. This effect is evident for process air flow rate changes at Run Hours 51 and 55.

RAH tube surface temperatures ranged from nominally 1370° to 1980°F (744° to 1083°C). The low end of the temperature range represents the back side of the tube surfaces near the process air inlet, with the high end of the temperature range representing the front side of the tube surfaces near the process air outlet. Changes in process air flow rates had noticeable effects on all tube surface temperatures. Tube surface temperature step changes were most noticeable for surface temperature measurements near the process air exit and on the front side of the tubes. Tube surface temperatures in February were comparable to all previous bituminous coal-fired tests, yet somewhat higher (10° to 40°F/6° to 22°C) than the temperatures observed in January.

Process air inlet temperature ranged from 1140° to 1190°F (616° to 644°C) but was nominally 1170° to 1190°F (633° to 666°C) for most of the coal-fired operational period. Outlet process air temperatures ranged from nominally 1650° to 1790°F (899° to 977°C). The effect of process air flow rate can be seen in the process air outlet temperature data. As process air flow rate decreases, process air exit temperature increases, as expected. These process air flow rate changes are noted at Run Hours 51 and 55. At Run Hours 34 and 41, a step increase in the process air inlet temperature results in a comparable increase in the process air outlet temperatures for a process air flow rate of 200 scfm (5.7 m^3/min).

Heat recovery data from the RAH panel are presented in Figure 3-53 for the February test. At process air flow rates of 180 and 200 scfm (5.1 and 5.7 m^3/min), the heat recovered from the RAH panel during coal firing was 131,730 to 134,615 Btu/hr (138,975 to 142,019 kJ/hr) and 132,690 to 140,385 Btu/hr (139,988 to 148,106 kJ/hr), respectively. For process air flow rates of 180 and 200 scfm (5.1 and 5.7 m^3/min), the heat recovery ranges are a function of minor adjustments to the coal feed rate and combustion air flow rates. The main burner firing rate was nominally 2.1 to 2.3 MMBtu/hr (2.2 to 2.3 × 10^6 kJ/hr).

A comparison of the RAH panel data for the February Kentucky bituminous coal-fired test and the January test firing Illinois No. 6 bituminous coal indicates a similar heat recovery rate. Although the low end of the ranges were higher during the February test. Again, these heat recovery rates are higher compared to bituminous coal-fired test periods in 1997 and 1998 where heat recovery rates in the RAH panel were typically <120,000 Btu/hr (<126,600 kJ/hr). As

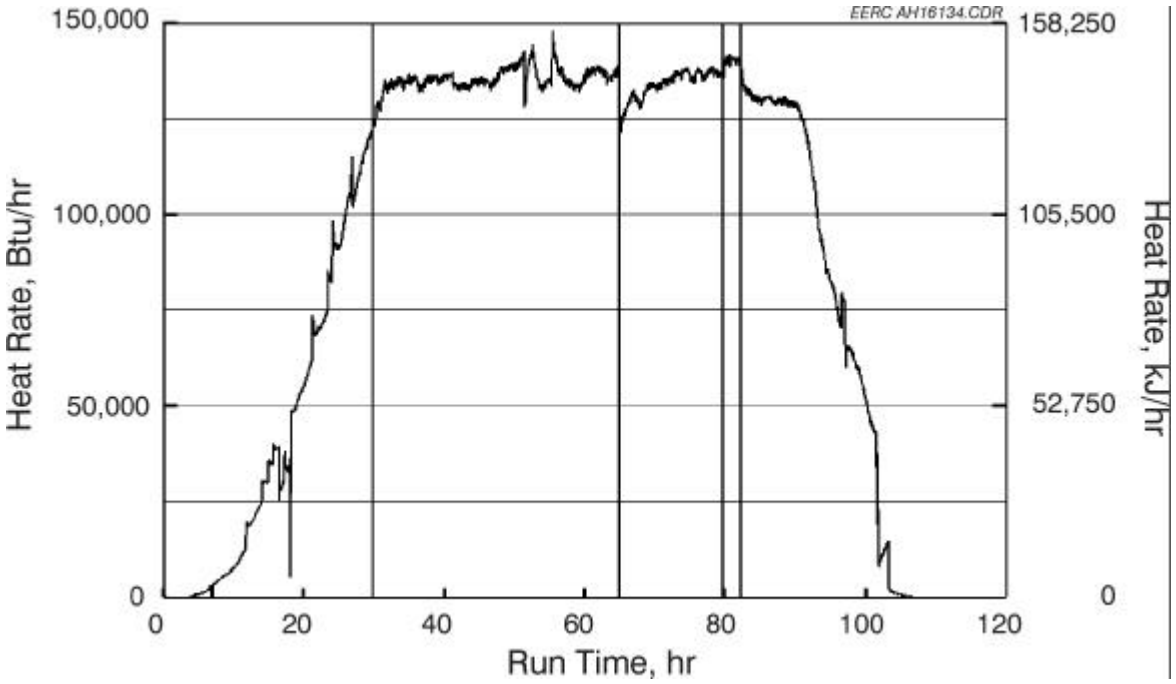

Figure 3-53. RAH heat recovery versus run time for the February test, SFS-RH7-0299.

previously stated in reference to the January data, the higher heat recovery rate observed in February was probably a function of many factors.

Figures 3-54 through 3-56 summarize the RAH ceramic tile temperatures, tube surface temperatures, and process air temperatures for the April test (SFS-RH8-0399). The process air flow rate data for the RAH panel were summarized in Figure 3-35. The indicated ceramic tile surface temperatures (cavity-side) ranged from nominally 2000° to 2140°F (1094° to 1171°C), based on measurements made at the center of each of the three large tiles once the SFS had stabilized thermally (Run Hours 50 through 248). Higher tile surface temperatures (furnace-side), 2400° to 2630°F (1316° to 1444°C), were measured near the center of the large middle tile. Tile surface temperatures during the April test were somewhat lower than the temperatures observed during the RAH coal-fired tests in January and February. Also, there is no obvious explanation for the drop in the furnace-side tile surface temperature that occurred just prior to Run Hour 100. One possibility is the degradation of the thermocouple junction as a result of slag erosion/corrosion of the tile surface. The thermocouple must be effectively attached and measuring a relative furnace-side temperature or the reading would have decreased to a value at or below the values indicated by TC19, TC22, and TC25 (cold/cavity-side tile surface temperatures).

RAH process air flow rates during the April test were controlled at 180, 190, and 200 scfm (5.1, 5.4, and 5.7 m^3/min), with 200 scfm (5.7 m^3/min) used primarily. Changes in process air flow rates had a definite effect on indicated tile surface temperatures as observed for the January

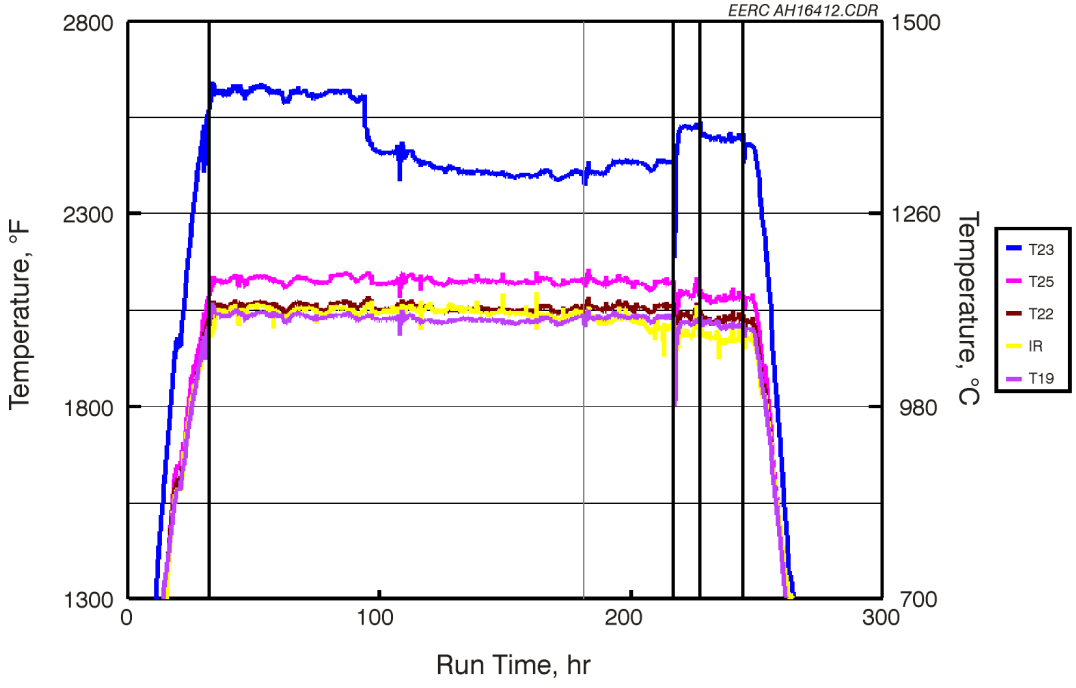

Figure 3-54. RAH ceramic tile temperatures versus run time for the April test, SFS-RH8-0399.

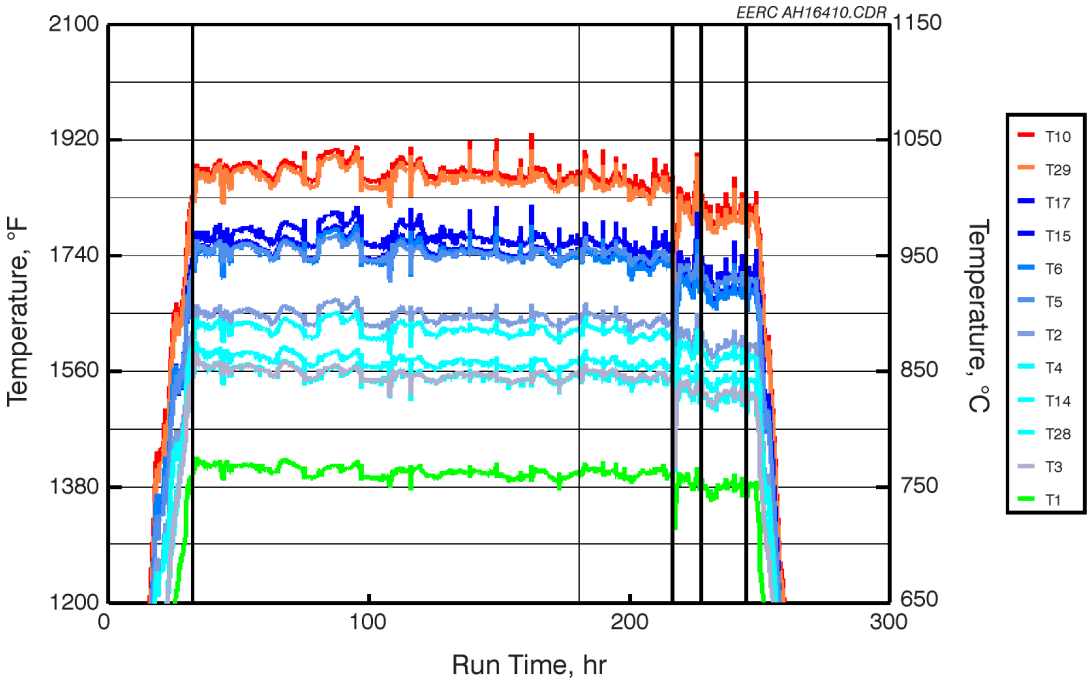

Figure 3-55. RAH tube surface temperatures versus run time for the April test, SFS-RH8-0399.

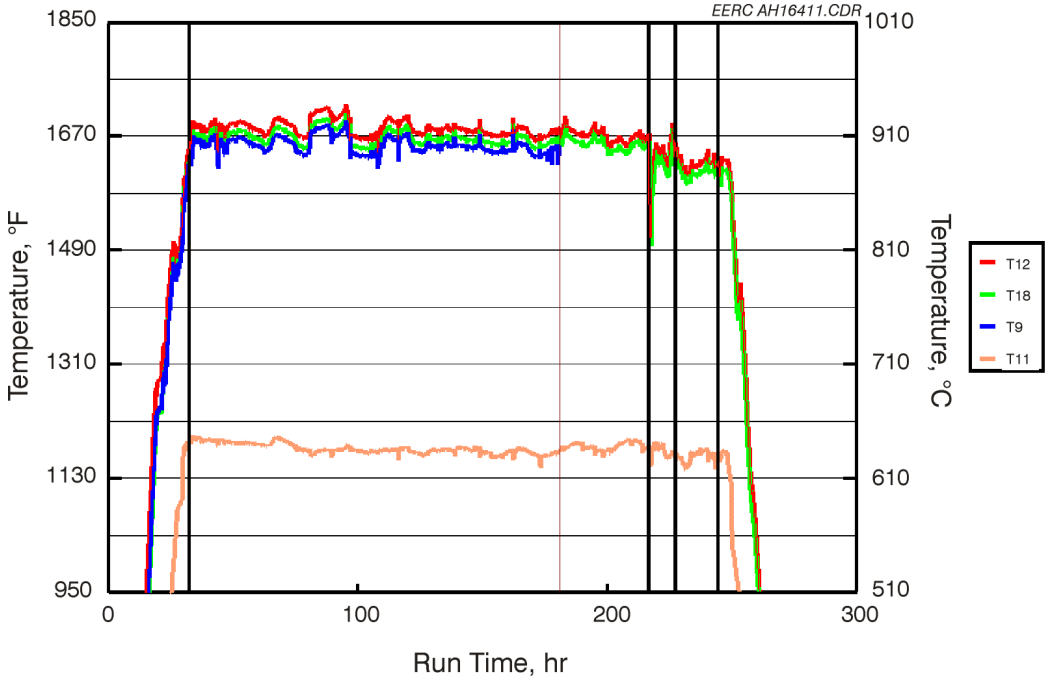

Figure 3-56. RAH process air temperatures versus run time for the April test, SFS-RH8-0399.

and February tests. This effect is most evident for process air flow rate changes at Run Hours 80, 95, 109, and 200.

RAH tube surface temperatures ranged from nominally 1390° to 1900°F (755° to 1038°C). The low end of the temperature range represents the back side of the tube surfaces near the process air inlet, with the high end of the temperature range representing the front side of the tube surfaces near the process air outlet. Changes in process air flow rates had noticeable effects on all tube surface temperatures. Tube surface temperature step changes were most noticeable for surface temperature measurements near the process air exit and on the front side of the tubes. Tube surface temperatures in April were comparable to all previous bituminous coal-fired tests, yet somewhat lower on the high end of the range when compared to the February data.

Process air inlet temperatures ranged from 1145° to 1195°F (619° to 646°C) but was nominally 1160° to 1190°F (644° to 666°C) for most of the coal-fired operational period. Outlet process air temperatures ranged from nominally 1610° to 1710°F (877° to 932°C). The effect of process air flow rate can be seen in the process air outlet temperature data. As process air flow rate decreases, process air exit temperature increases, as expected. These process air flow rate changes are noted at Run Hours 80, 95, 109, and 200.

Heat recovery data from the RAH panel are presented in Figure 3-57 for the April test. At process air flow rates of 180, 190, and 200 scfm (5.1, 5.4, and 5.7 m^3/min), the heat recovered from the RAH panel during Kentucky coal firing was 115,385 to 118,750 Btu/hr (121,731 to 125,281 kJ/hr), 115,385 to 119,710 Btu/hr (121,731 to 126,294 kJ/hr), and 120,670 to

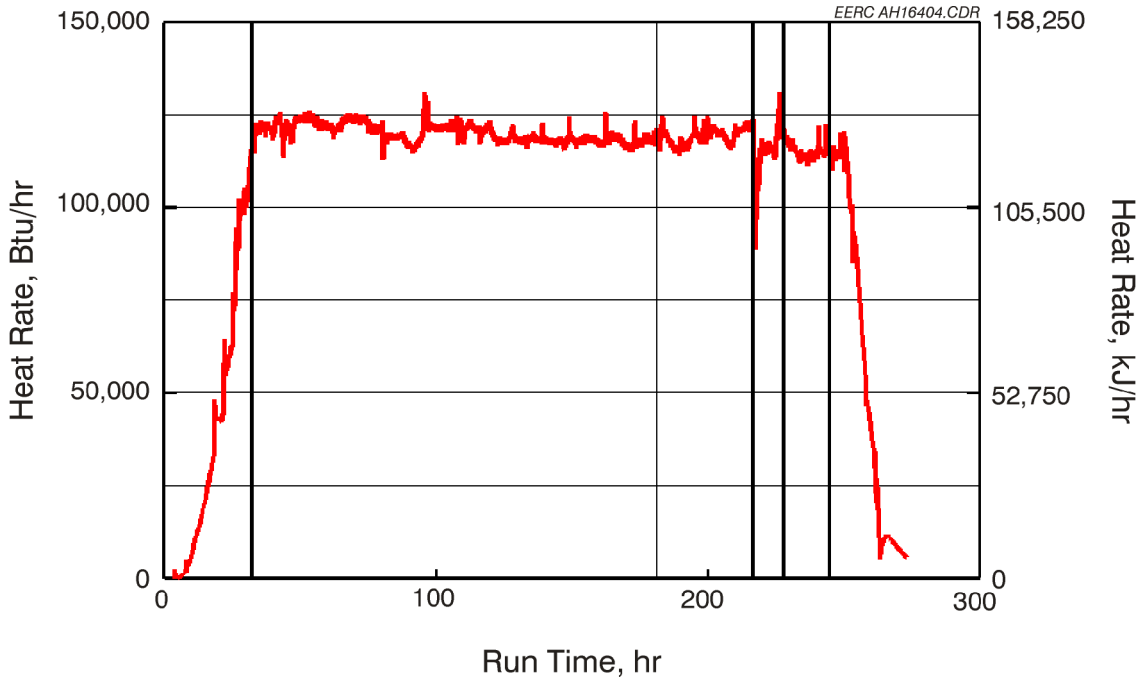

Figure 3-57. RAH heat recovery versus run time for the April test, SFS-RH8-0399.

125,000 Btu/hr (127,307 to 131,875 kJ/hr), respectively. The heat recovery ranges are a function of minor adjustments to the coal feed rate and combustion air flow rates. The main burner firing rate was nominally 2.1 to 2.3 MMBtu/hr (2.2 to 2.4 × 10^6 kJ/hr). Based on the RAH heat-transfer data obtained during the three test periods completed, no conclusion can drawn concerning the use or nonuse of a coating on the cavity side of the RAH ceramic tiles to improve cavity-side heat transfer.

A comparison of the RAH panel data for the April eastern Kentucky bituminous coal-fired test and the February test firing the same fuel indicates that there was a significant decrease in the heat recovery rate. The decrease appears to be 10% to 15%. During the February test, the heat recovery rate in the RAH panel was 131,730 to 140,385 Btu/hr (138,975 to 148,106 kJ/hr). However, the heat recovery rate observed in April was somewhat higher than the heat recovery rate observed during slagging furnace test periods in 1997 and 1998. EERC personnel believe that the lower heat recovery rate observed in April when compared to February may be the result of the aging of the high-density refractory in the furnace, specifically related to the darkening of the refractory and a potential reduction in its reflectivity.

Figure 3-58 presents heat recovery data for the RAH panel resulting from bituminous coal-fired tests and process air flow rates of 180 and 200 scfm (5.1 and 5.7 m^3/min). The data in the figure show that the lowest heat recovery rate was observed in February 1998 (RH3), with the highest heat recovery rate observed in February 1999 (RH7). Because of slight differences in slagging furnace configuration (the presence or absence of the SRAH panel and water-cooled blank door), direct comparisons of RAH heat recovery are only valid for tests completed in the

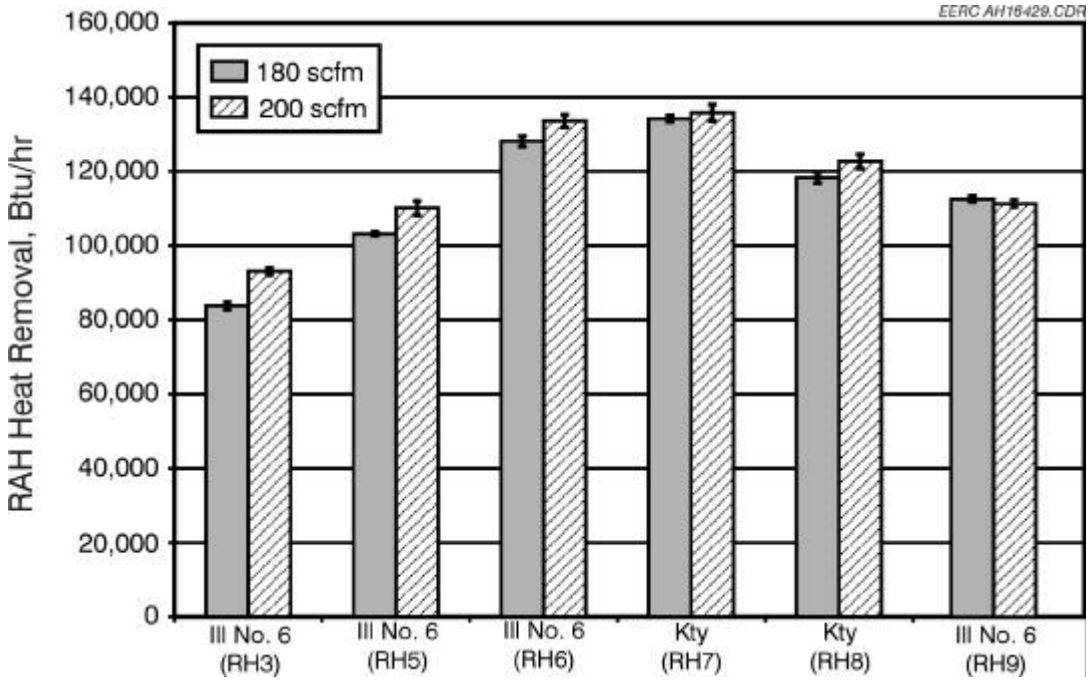

Figure 3-58. RAH heat recovery for bituminous coal-fired tests completed in 1998 and 1999.

past 6 months (RH6, RH7, RH8, and RH9). Specifically, a comparison of RH7 and RH8 (firing eastern Kentucky coal) shows a decrease in the RAH panel heat recovery rate. These data indicate that the heat recovery rate for the RAH panel is decreasing with each week of operation since the slagging furnace high-density refractory was replaced in late 1998 and the RAH panel was reassembled in January 1999. A comparison between RH6 and RH9 data also support this conclusion. RH9 data are the result of a test completed in May 1999 (SFS-RH9-0499) in support of the Combustion 2000 HiPPS program.

EERC personnel believe that one or two possible factors are causing this change in RAH panel performance relative to heat transfer from the furnace to the radiation cavity. One possibility is a potential change to the RAH ceramic tiles resulting in a decrease in the heat transfer to the radiation cavity. The flame-side surface of the RAH ceramic tiles did darken as a result of slag coating and absorption during the January 1999 test. However, it is not clear what the effect would be on radiant heat absorption or emission, or thermal conductivity. Also, no additional color changes were noted following subsequent test periods. In addition, the changing heat transfer may be related to the tile deterioration with each week of coal-fired furnace operation as a result of slag erosion/corrosion. Erosion/corrosion of the ceramic tiles may be affecting their heat-transfer properties.

Another potential contributing factor to the decreasing heat transfer may be the high-density furnace refractory color change observed with each week of operation. As the high-density refractory has darkened with each week of operation, it is possible that the reflectivity, emissivity, or conductivity of the furnace liner has changed, resulting in a decrease in radiation to the RAH panel. Further testing and data review will be necessary to determine if the observed decrease in RAH panel heat recovery rate continues with each week of testing or if an alternate explanation can be identified.

With completion of the April test, the RAH panel had been exposed to a range of furnace-firing conditions for a total of 1485 hours. Natural gas firing represented 801 hours, and coal/lignite firing represented 684 hours. In addition, the RAH panel was exposed to ten heating and cooling cycles. The RAH ceramic tiles that were installed in January 1999 were exposed to three heating and cooling cycles and 480 hours of slagging furnace operation: 181 hours of natural gas firing (including heatup and cooldown) and 299 hours of coal firing. The longest continuous coal-fired period was 184 hours, completed in April 1999.

3.2 Laboratory- and Bench-Scale Activities

3.2.1 Dynamic Slag Corrosion Testing

Modifications were made in the way that the castable refractory blocks are prepared, and four refractory blocks were tested for corrosion resistance in the DSAF during the course of this project. Two modifications were made to the castable blocks to reduce the amount of slag that adheres and flows back under the block where it drips into the furnace rather than out of the exit port. The area directly behind the drip lip was deepened, and a piece of nonwetting platinum foil was attached to the base of the drip lip. A third modification was to deepen the slag well at the

top of the block to allow the slag to pool longer before flowing down the vertical channel. This is especially important later in a test when the exit from the slag pool is corroded, allowing the slag to flow out of the pool too rapidly.

The four refractory blocks tested in the DSAF during this project included three blocks of the experimental Plicast 98 alumina castable prepared and fired to 2958°F (1625°C). Two of them were coated with materials in order to reduce the penetration of slag between the grains. In one case, the slag pool and flow channel were coated with a mixture of colloidal alumina and silica, and for the second block, a suspension of submicron alumina powder was used. The third block was left uncoated as a control. In addition to testing the three castable refractory blocks, a sintered high-alumina material containing 10%–12% chromia, supplied by Kyocera to UTRC, was tested. All of the corrosion tests were performed with Illinois No. 6 slag at 2732°F (1500°C). The airflow rate into the furnace was also reduced from 125 cm^3/min (0.004 ft^3/min) per entry port to approximately 12.5 cm^3/min (0.0004 ft^3/min) to reduce the amount of rebound and splash when the unmelted slag particles drop onto the top of the test block.

During the nominally 100-hour tests, slag dripped freely from all of the blocks and did not flow back along their bottoms into the furnace. Surface recession measurements were made on each block after testing. Figure 3-59 is a plot comparing the recession rates with time for the sintered chrome–alumina brick as compared to the fusion-cast Monofrax L and M bricks which were tested previously. Monofrax M is the material used to make the tiles on the front of the LRAH. The plot shows the chrome–alumina refractory had a much lower recession rate than either of the Monofrax materials, although it was found after the tests that there was some variation in slag feed rates during the tests. The feed rate during the chrome–alumina test was

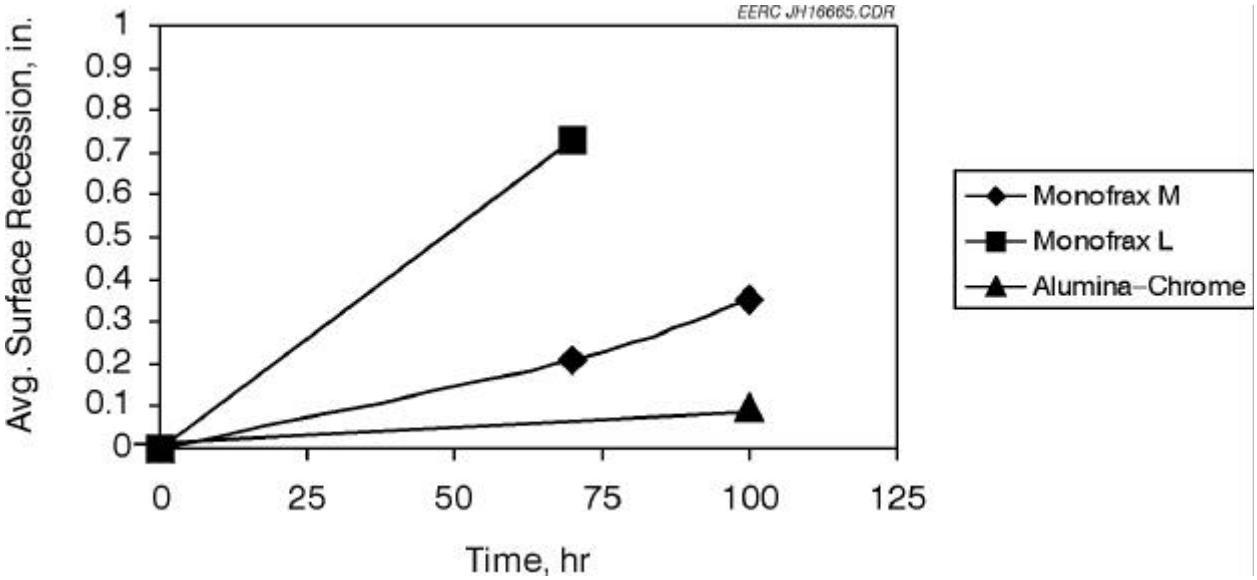

Figure 3-59. Graph of recession with time for the sintered chrome–alumina refractory and the alumina-based fusion-cast Monofrax L and M, tested with Illinois No. 6 slag at 2732°F (1500°C).

approximately 0.09 lb/hr (41 g/hr) per entry port, compared to approximately 0.11 lb/hr (51 g/hr) per entry port when the Monofrax L and M were tested with Illinois No. 6 slag.

Figure 3-60 is a photograph of the chrome–alumina block after 103 hours of slag feed. The photograph shows that the surface of the block has only slightly receded and the discoloration caused by slag penetration into the block, on either side of the vertical channel, is minimal. The erosion of the chrome–alumina block was mainly concentrated at the center, creating a v-shaped channel instead of the usual broad u-shape observed in the Monofrax M block, as shown in Figure 3-61. After 103 hours of slag feed, the chrome-containing block had an average measured recession of 0.09 in. (0.23 cm), which is a rate of 0.0009 in./hr (0.0023 cm/hr). This is a 70% reduction compared with 0.35 in. (0.89 cm) (0.003 in./hr or 0.001 cm/hr) for Monofrax M and a 91% reduction compared to the 0.73 in. (0.29 cm) (0.01 in./hr or 0.004 cm/hr) after 70 hours for Monofrax L. In addition, because of the difference in corrosion channel shapes, the relative volume loss by the chrome–alumina material was much less than the ratios of recession depths would indicate. The much more narrow erosion channel for the chrome–alumina bricks should also substantially reduce the formation of slag flow rivulets that focus the slag corrosion of the Monofrax M panels in the SFS. The recession would most likely have been slightly higher for the chrome–alumina refractory at a slag feed rate of 0.11 lb/hr (51 g/hr), but it is still apparent this refractory holds up very well in the presence of flowing slag.

To address environmental issues related to the disposal of chrome-containing refractories and their spent slag, chemical analysis using TCLP (toxicity characteristic leaching procedure), EPA Test Method 1311, has been completed on a sample of spent slag from the chrome–alumina

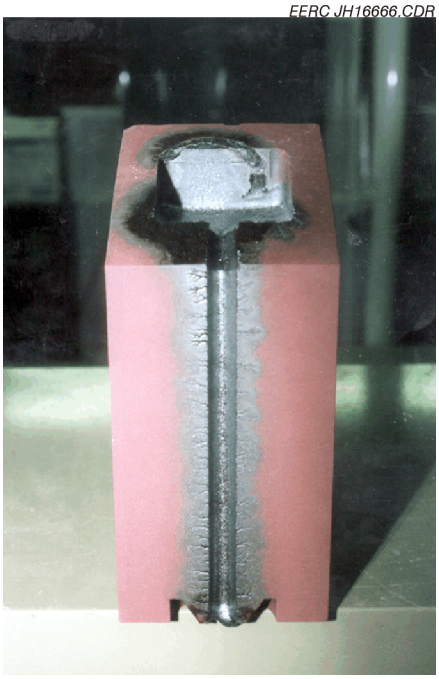

Figure 3-60. Photograph of the chrome–alumina block from UTRC after 103 hours of slag feed at 2732°F (1500°C) using Illinois No. 6 slag.

Figure 3-61. Photograph of the Monofrax after 100 hours of slag feed at 2732°F (1500°C) using Illinois No.6 slag.

fusion cast material. The spent slag sample was collected after 9 hours of slag feed. The leachate contained approximately 5 µg of chrome per liter. The measured value is three orders of magnitude below the EPA disposal limit of 5 mg/L and one order of magnitude below the drinking water limit of 50 µg/L. Wavelength-dispersive x-ray fluorescence (WDXRF) analyses were done on two spent slag samples for the chrome–alumina refractory and Plicast 98 materials to determine the amount of chrome removed from the chrome–alumina refractory and to monitor the remaining oxide concentrations. The spent slag samples were collected from the water quench vessel. The first sample was taken after 9 hours of slag feed, and the second was taken at the end of the test, after 103 hours of slag feed. Table 3-10 summarizes the compositions for the slag (Illinois No. 6) and the refractory reactant products as a function of slag flow time.

In general, the numbers stayed fairly constant for both refractory samples. Very little chrome was removed from the chrome–alumina refractory. The greatest changes in oxide concentrations were found in silica and alumina in the slag reactant product for the coated Plicast 98 sample. The silica decreased from 53.8% to 50.6%, and the alumina increased from 19.0% to 21.5% after 103 hours of slag feed. These results are typical, as the recession was also higher for the Plicast 98 material (0.28 in. or 0.71 cm) than the chrome–alumina sample (0.09 in. or 0.23 cm). It was found in previous tests using the Plicast materials, because of their higher porosity than the brick samples, that the silica is lost through penetration into the refractory and the alumina is removed from the refractory material and dissolved into the slag.

Figure 3-62 is a photograph of Plicast 98, an experimental 98% alumina castable developed in cooperation with the Plibrico company, that was prefired to 2957°F (1625°C) and tested at

TABLE 3-10

Illinois No. 6 Slag and Slag Reactant Product Compositions as Determined by WDXRF

Oxides, wt%	Illinois No. 6 Slag, as-received	9-hour Slag Chrome–Alumina	103-hour Slag Chrome–Alumina	9-hour Slag Coated Plicast	103-hour Slag Coated Plicast 98
SiO_2	54.4	52.4	52.0	51.6	50.6
Al_2O_3	19.0	19.3	19.3	20.0	21.5
Fe_2O_3	15.6	16.5	16.8	16.5	16.4
TiO_2	0.7	0.9	0.9	0.9	0.8
P_2O_5	0.0	0.2	0.2	0.2	0.2
CaO	7.1	6.5	6.6	6.5	6.4
MgO	1.3	1.7	1.8	1.8	1.8
Na_2O	0.0	0.6	0.6	0.6	0.6
K_2O	1.8	1.8	1.8	1.9	1.8
SO_3	0.0	0.0	0.0	0.0	0.0
Cr	0.0	0.06	0.07	0.02	0.02

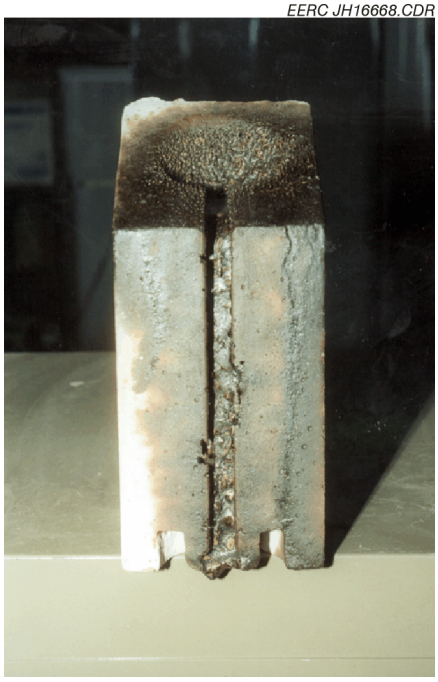

Figure 3-62. Photograph of the coated Plicast 98 material that was prefired to 2957°F (1625°C) and tested at 2732°F (1500°C) for 103 hours using Illinois No. 6.

2732°F (1500°C) for 103 hours using Illinois No. 6 slag. This block was coated with a paint consisting of a suspension of silica and alumina particles to help seal pores in the refractory. The corrosion is much more visible, and the discoloration caused by the slag penetration is much more extensive than with the chrome–alumina block or the Monofrax materials. The average recession after 103 hours of slag feed for the coated Plicast 98 sample prefired to 2957°F (1625°C) and tested at 2732°F (1500°C) was 0.28 in. (0.71 cm). This is compared to 0.62 in. (1.57 cm) after 54 hours of slag feed for a previously tested uncoated Plicast 98 sample prefired and tested at 2732°F (1500°C) shown in Figure 3-63. When comparing Figures 3-62 and 3-63, it is clear that the corrosion/erosion effects are much greater for the uncoated lower prefire-temperature block. The vertical channel is much rougher and more eroded than the coated block that was fired to the higher temperature. Overall, the coating and higher prefiring temperature dropped the corrosion rate by 75%,although as was mentioned with the chrome–alumina block, the feed rate was approximately 0.022 lb/hr (10 g/hr) less for this test. The small reduction in feed rate is not believed to be significant in causing the greatly reduced corrosion rate. It was not clear, however, whether the coating or the higher prefiring temperature were more responsible for the lower recession rate.

To differentiate between the effects of the coating from those due to the higher prefire temperature and to test another coating type, two additional Plicast 98 blocks were prepared, prefired to 2957°F (1625°C), and tested at 2732°F (1500°C). One of the blocks was painted with a suspension of alumina particles to seal the pores, and the other was left uncoated as a control to separate the effects of the coating from the higher prefire temperature. These two blocks were exposed for 90 hours in the DSAF at 2732°F (1500°C), using Illinois No.6 coal

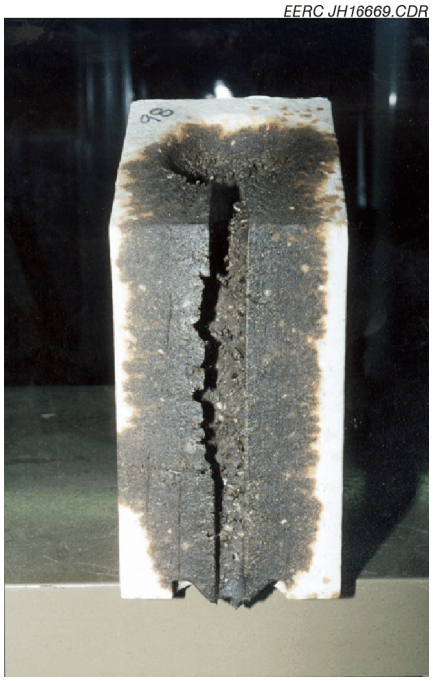

Figure 3-63. Photograph of uncoated Plicast 98 material that was prefired and tested at 2732°F (1500°C) for 54 hours using Illinois No. 6 slag.

slag. The feed rate was approximately 0.11 lb/hr (50 g/hr) per entry port. The block with the painted corrosion-resistant coating had an average measured recession of 0.34 in. (0.86 cm), and the uncoated block had an average measured recession of 0.29 in. (0.74 cm). The slightly higher recession for the block with the paint-on coating shows that this coating was not effective in reducing the corrosion rate with Illinois No. 6 slag, although it may still increase corrosion resistance to more alkaline coal slags. Figure 3-64 is a graph showing the recession depths of the different Plicast 98 blocks. It shows that prefiring to 2910°F (1625°C), rather than 2732°F (1500°C), reduced the corrosion by 70%, and that neither coating increased corrosion resistance to the Illinois No. 6 slag. However, the coatings may be more effective with more basic slags.

3.2.2 Effect of Additives on Slag Viscosity

Proper slag flow and slag corrosion are major operational concerns for the HITAF. Since the viscosity for the slag controls its flow characteristics as well as the rate of mass transport of corrodents, it is important to delineate the factors affecting slag viscosity so that accurate predictions of flow and corrosion in different regions of the HITAF can be made. The factors affecting viscosity include slag composition, local atmosphere, and slag temperature. The variable over which the operator has the most control is composition through coal selection or the use of additives. By manipulating the composition of the slag, it may be possible to control slag behavior in ways such as ensuring slag flow through taps or reducing the corrosiveness of the slag by reducing the rate of mass transport of corrodents to the refractory.

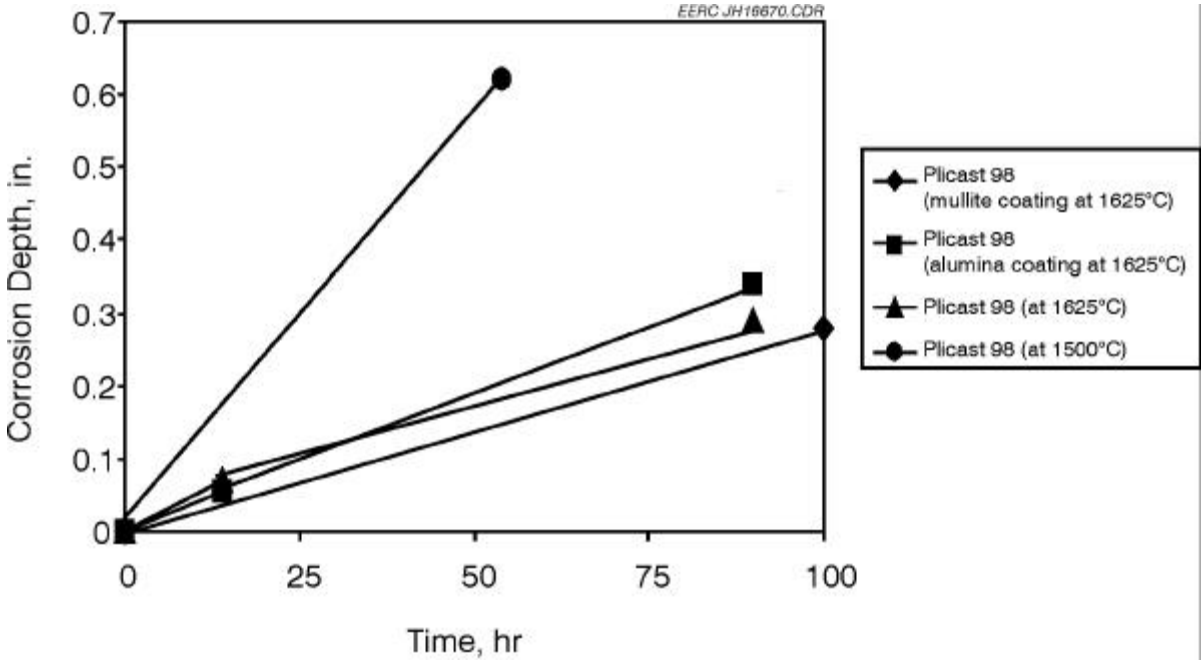

Figure 3-64. Plot of recession versus time for Plicast 98 castable material with and without corrosion-resistant coatings.

During this project, changes in viscosity-versus-temperature curves were determined for the Rochelle subbituminous slag for which data have been previously reported and a slag formed in the SFS while CCS lignite was tested in April 1998. The tests were performed under simulated coal combustion conditions as functions of additive composition. These measurements were repeats of others reported in earlier quarterly technical progress reports to show the effects of changes in test procedures on the measured data.

A test matrix was developed to plot the effect of the addition of alumina, calcia, or silica on the viscosity-versus-temperature curves for both slag sources. The test matrix included mix proportions at 10 wt% of each additive. This level of additive should have a minute economic impact on the operation of a HITAF, since a 10 wt% addition on a slag basis is approximately one-fifth of the relative addition on a coal basis as compared to the addition of limestone for capturing sulfur in a pressurized fluidized-bed combustor (PFBC). Also, the additives used in a HITAF melt into the slag and are easily disposed of, even sold as a commercial product, as compared to the highly leachable bed materials produced from a PFBC which are difficult to dispose.

The slags for the viscosity measurements were prepared by first grinding the slag to a −20-mesh (−8.33-µm) size. A total of 0.22 lb (100 g) of the powdered slag with the appropriate amount of the selected additive oxide was placed in an attrition mill with about 200 mL of isopropanol. The slag slurry was mixed and milled for 1 hour. The slurry was then vacuum-dried and placed in a drying oven at 140°F (60°C) for about 24 hours. The slags were prepared by melting each ash or ash–blend in air in a platinum crucible and then quenching them on a brass plate at room temperature. The slags were crushed, placed in a platinum/rhodium crucible, and reheated to 2732°F (1500°C) to start and the viscosity measured as the temperature was dropped, holding at each temperature until the viscosity stabilized.

Modifications to the viscosity testing procedure were incorporated to better ensure the testing environment was closed to outside contaminants. First, platinum–rhodium crucibles were used instead of alumina which had been used in the past. It was determined earlier that measurable amounts of alumina were dissolving into the slag, which consequently could affect the viscosity measurements. This was considered a potential problem generally while testing slags from lignite and subbituminous coals. The viscometer furnace is a box-type furnace with an alumina tube aligned from the top to the bottom of the furnace. The tube exiting out the bottom of the furnace is sealed with a cap. This is designed to prevent outside gases from entering, as well as minimizing the test gas mixture from seeping out of, the test chamber environment. In addition, an electric steam generator is now being used to regulate the moisture output into the test gas mixture.

Viscosities were measured with a Haake Viscometer® VT550 system which uses a rotating-bob viscometer. The bob, which is made of platinum, is 9 mm in diameter and 20 mm long and has a 45 degree taper at each end. It is submerged into the slag until the slag just covers its top, and then it is rotated at 45.3 rpm. The torque applied to the viscometer is read and converted to an electrical signal that is sent to a computer with a data acquisition program that determines the viscosity of the slag. The viscosity of the slag was measured over the range of 45 to as high as 280 poise unless crystallization was seen to occur along the walls of the alumina container, at

which point the measurement was terminated. In all cases, crystallization occurred before higher-viscosity measurements were possible. Viscosities over 1000 poise are certainly attainable with the VT550 system. The viscometer was calibrated with National Bureau of Standards silicate glass 710a. The accuracy of the viscosity test is approximately 5%. The tests were run in an oxidizing gas environment of 13% CO_2, 4% O_2, 1000 ppm SO_2, and 10% H_2O with a nitrogen balance.

Figure 3-65 shows the viscosity-versus-temperature curves for two repeat measurements of the original Rochelle slag. The figure indicates that the temperature at which the slag has a viscosity of 250 poise, or T_{250}, is approximately 2192°F (1200°C), although this measured temperature can vary up or down by 54°F (30°C) between tests. 250 poise is a benchmark value because at higher viscosities the slag does not flow easily from a combustor. This variability is often seen in more basic slags because they are prone to rapid solidification which is difficult to reproduce. Figure 3-66 shows the viscosity-versus-temperature curves for the original Rochelle slag and the three modified Rochelle slags. The curves indicate that the additions of 10% silica or alumina to the slag have insignificant impacts on the T_{250}, although the alumina addition may increase the propensity for the slag to solidify suddenly upon cooling. The addition of calcia, however, substantially reduces the T_{250} of the slag. This is in contrast to the data measured previously when an alumina crucible was used, which showed that the addition of calcia dropped the T_{250} of the slag only slightly, whereas the addition of alumina and silica greatly increased the T_{250}. The difference in behavior is most likely an indication of the effect of the dissolution of a

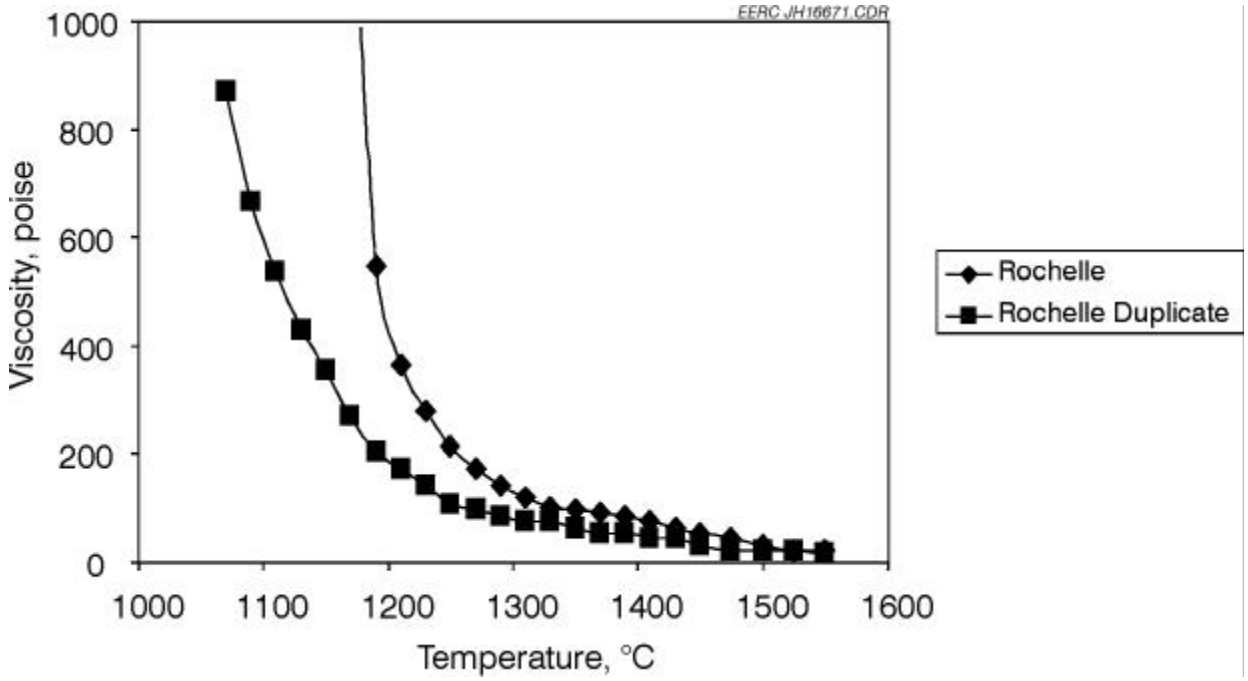

Figure 3-65. Viscosity-versus-temperature curves for two repeat measurements of the Rochelle slag.

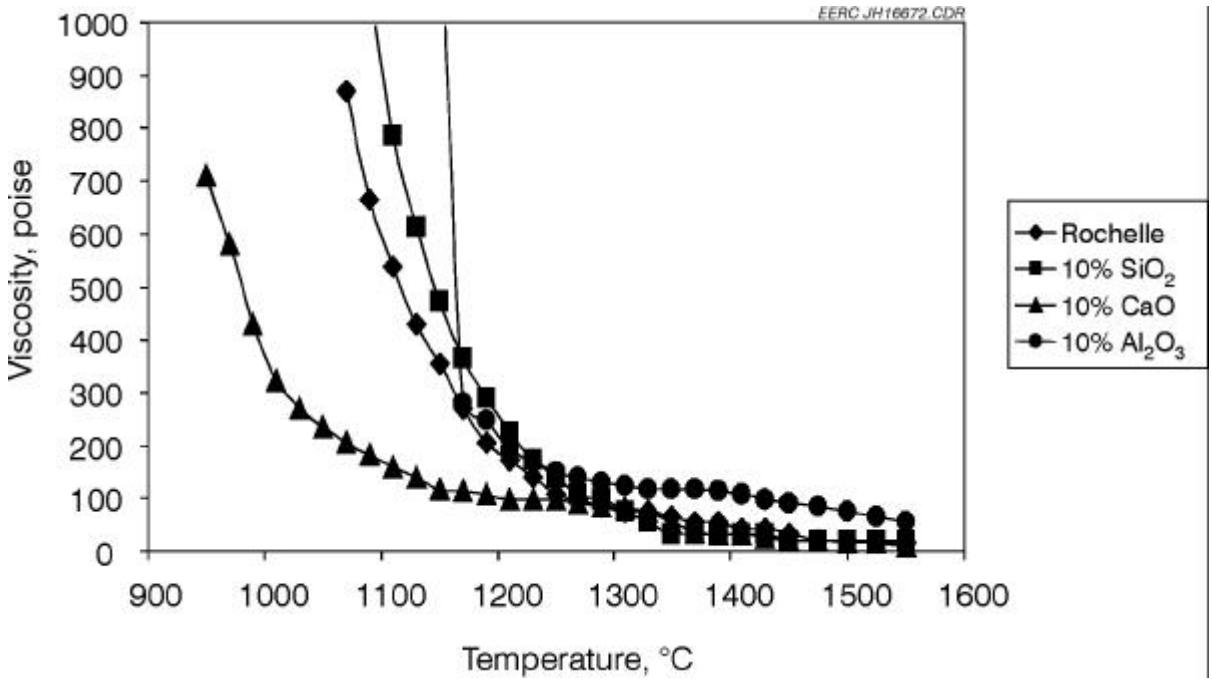

Figure 3-66. Viscosity-versus-temperature curves for the original and modified Rochelle slags.

small amount of the alumina crucible into the slag in the earlier test, which substantially increased the alumina content of the slag above that attributable to the additive.

Figure 3-67 shows the viscosity-versus-temperature curves for the slag produced in the SFS while the CCS lignite was fired in April of 1998 under separate funding. It indicates that the lignite slag has a T_{250} approximately 270°F (150°C) lower than that of the Rochelle slag. The addition of calcia to the lignite slag appears to slightly reduce the $T_{250,}$ whereas the addition of alumina and silica appears to slightly increase it, although the changes are on the order of the natural variability in the measurement. As was also true for the addition of the alumina to the Rochelle slag, adding alumina to the lignite slag increases its propensity to rapidly solidify near the T_{250}.

3.2.3 Heated-Stage XRD Analysis of Slags

In order to develop a better model of the viscosity-versus-temperature behavior of coal slags, it is necessary to understand the temperature-related crystallization behavior of the slags. To determine the temperature-versus-crystallization behavior of coal slag, a heated-stage x-ray diffraction system is being used. It employs a Philips X'Pert-MPD x-ray diffraction system utilizing a PW3040 console. Attached is a removable Buhler HDK 1.4 high-temperature chamber (heated stage). This system arrangement, called theta–theta, allows the sample to sit still in the heated-stage chamber while the x-ray source and detector rotate about an arc, allowing the sample to be heated to the melting point. The high-temperature chamber consists of a cylindrical,

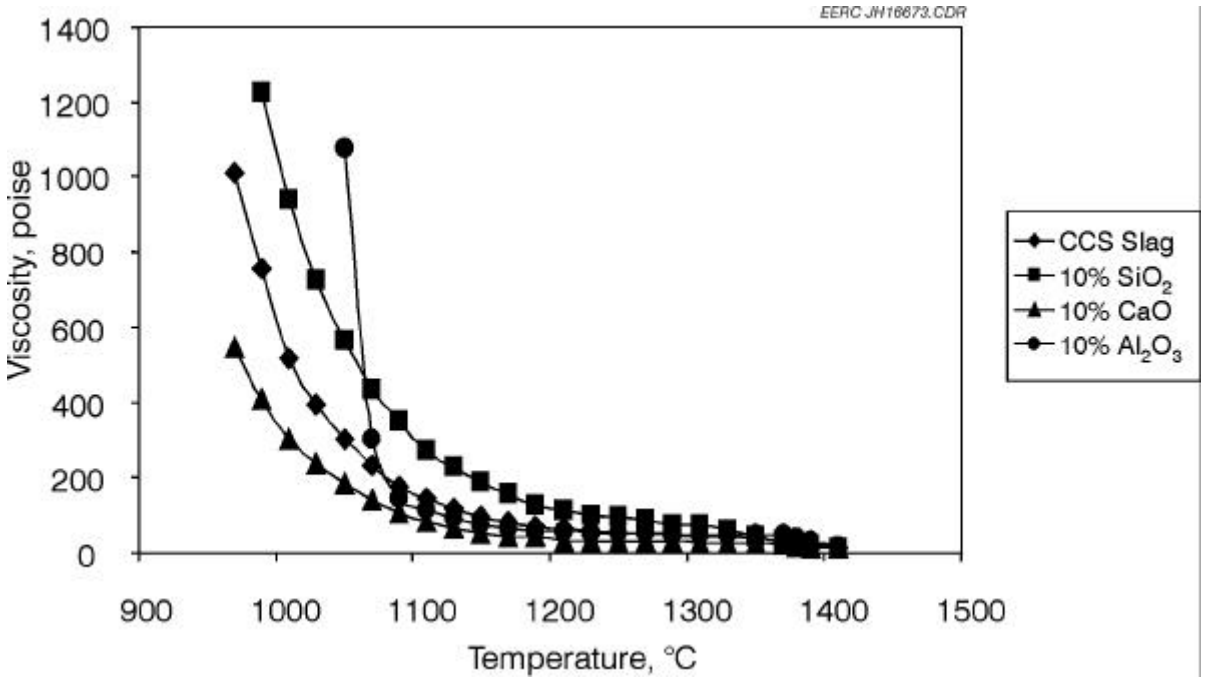

Figure 3-67. Viscosity-versus-temperature curves for the original and modified CCS lignite slag and modified slags.

double-walled, water-cooled pot made of stainless steel. It is equipped with a beryllium irradiation window and ports for a vacuum/pressure pump and inlet/outlet gases. The sample rests in a depression of a metal strip composed of platinum–rhodium alloy, connected to a power source and controlled by means of a thermocouple physically attached to the sample strip. A computer and software ultimately control the entire diffraction system.

During testing, the sample was heated using a ramp rate of 90°F (50°C) per minute to testing temperatures of 932°, 1832°, 2192°, 2282°, and 2372°F (500°, 1000°, 1200°, 1250°, and 1300°C) and then in increments of 45°F (25°C) to 2912°F (1600°C). Upon cooling, the testing temperatures were in increments of 45°F (25°C) from 2912°F (1600°C) to 2102°F (1150°C), 2012°, 1922°, 1832°, 1472°, and 932°F (1100°, 1050°, 1000°, 800°, 500°C). The system was allowed to equilibrate for 1 minute before scanning. A synthetic combustion gas composed of 14% CO_2, 4% O_2, and 1000 ppm SO_2, with the balance N_2, was introduced into the chamber at a rate of 2 scfh (0.06 m^3/hr). Steam was also introduced as a mass fraction of 10% of the gas or 0.2 scfh (0.006 m^3/hr).

Under this project, three samples of slags collected from the SFS after the February test of the eastern Kentucky coal were analyzed. X-ray diffraction scans were taken at each temperature interval during heating and also during cooling. The scans were then qualitatively analyzed, noting the presence and/or absence of phases as they related to temperature.

Figures 3-68 and 3-69 show the changes in x-ray diffraction patterns for a sample of slag collected from the slag tap while heating to the melting point, then cooling, respectively. At room temperature, the identified crystalline phases were mullite ($Al_6Si_2O_{13}$), hercynite ($FeAl_2O_4$), and hematite (Fe_2O_3). At 1832°F (1000°C), hercynite assimilated into the melt, and a transition phase of plagioclase [(Ca, Na)(Al, Si)$_4O_8$] was detected, which was not detected above 2462°F (1350°C). Hematite assimilated into the melt at 2642°F (1450°C). By 2822°F (1550°C), the entire sample had melted. When cooling, mullite crystallization could not be detected until 2507°F (1375°C). Hematite crystallization was detected at 2012°F (1100°C), and by 1922°F (1050°C), hercynite could also be detected. Plagioclase did not form during cooling.

Results of analyses of two samples from the slag screen were only slightly different from the slag tap sample. At room temperature, the only detected crystalline phases were mullite and hercynite. Hematite was detected at 1832°F (1000°C) and plagioclase at 2192°F (1200°C). By 2372°F (1300°C), hercynite, hematite, and plagioclase could not be detected. At 2867°F (1575°C), the sample was completely melted. During cooling, mullite crystallization could be detected at 2507°F (1375°C). At 2012°F (1100°C), hercynite was detected, and by 932°F (500°C), hematite could also be detected but did not appear to be present at room temperature. Again, plagioclase did not form during cooling.

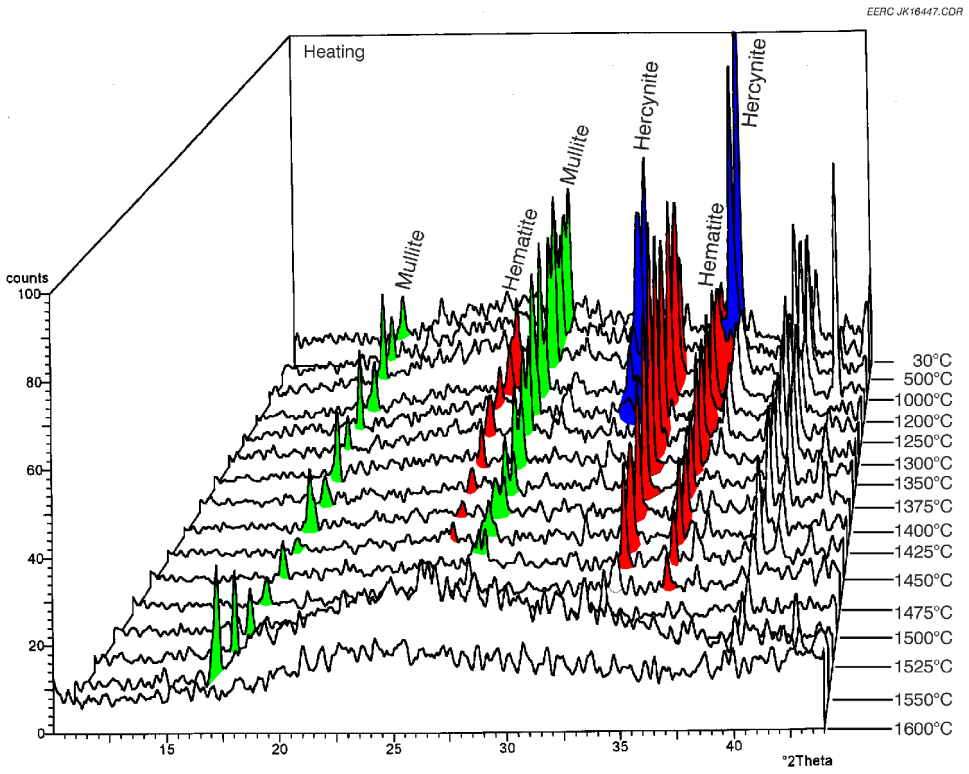

Figure 3-68. X-ray diffractograms for the eastern Kentucky slag tap sample measured while heating to the melting point.